

Magnitudes, Spatial Extent, Time Scales and Causes of Shoreline Change Adjacent to an Ebb Tidal Delta, Katikati Inlet, New Zealand

D. Murray Hicks, Terry M. Hume, Andrew Swales, and Malcolm O. Green

National Institute of Water
and Atmospheric Research
Ltd.
P.O. Box 8602
Christchurch, New Zealand

National Institute of Water
and Atmospheric Research
Ltd.
P.O. Box 11-115
Hamilton, New Zealand

ABSTRACT



HICKS, D.M.; HUME, T.M.; SWALES, A., and GREEN, M.O., 1999. Magnitudes, Spatial Extent, Time Scales and Causes of Shoreline Change Adjacent to an Ebb Tidal Delta, Katikati Inlet, New Zealand. *Journal of Coastal Research*, 15(1), 220-240. Royal Palm Beach (Florida), ISSN 0749-0208.

The ebb delta and adjacent beaches at a mixed energy (tide dominated) inlet were monitored to identify the influence of the inlet/ebb-delta system on erosion and accretion of the adjacent beaches. Sub-aerial beach profile data were collected at 25 locations at monthly intervals over four years. Beach excursion distances and volumes, dispersion diagrams, principal components analysis, and time-series correlations with wave parameters were used to extract the magnitudes, time scales, and causes of the beach changes. The divergence induced in the regional longshore transport regime by wave refraction over the ebb delta was also investigated. Changes on the adjacent beaches, beyond the wave shadow of the ebb delta and more than 3-4 km from the inlet centreline, were dominated by a quasi-annual signal which reflected cross-shore sand transport forced by storm waves. Lesser changes were linked with longshore transport, which reversed its prevailing direction at inter-annual time scales. The longshore transport caused sand oscillation between the small headlands bounding the western beach, sand inputs to the inlet/ebb-delta system from the beaches either side, and a standing pattern of erosion and accretion about the inlet due to refraction-induced transport divergence. Immediately behind the ebb delta the quasi-annual storm-wave signal was either small or non-discernible against much larger, multi-year changes. The multi-year changes correlated with the longshore transport potential and were interpreted as being associated with scouring by the marginal flood-tidal flows, accretion of sand bars migrating shoreward from the ebb delta platform and flanks, and longshore transport divergence. Most of these changes appeared to be the on-shore signature of part of a cycle of sand circulation between the beaches and the ebb delta bars.

ADDITIONAL INDEX WORDS: *Beach erosion, ebb tidal delta, tidal inlet, beach profiles, dispersion diagrams, principal components analysis, longshore transport, transport divergence, fall speed parameter, Southern Oscillation Index, coastal hazards.*

INTRODUCTION

Ebb tidal deltas are known to influence the stability of beaches adjacent to their inlets (see FITZGERALD, 1988, and FENSTER and DOLAN, 1996, for reviews). A thorough understanding and quantification of this influence is required when assessing coastal erosion hazards in the vicinity of tidal inlets. Key questions are: (i) "what is the magnitude of the beach changes; (ii) how do these changes vary alongshore away from the inlet; (iii) what time scales are represented in the various patterns of beach change; and (iv) what processes are causing the changes and what are the main forcing functions"? When defining erosion hazard zones on the basis of surveyed historical changes in shoreline position or shore sand volumes, the monitoring frequencies in space and time should match the actual temporal and alongshore scales of beach change, while any attempt to model the erosion hazard requires that the effects of the various processes be identified and separated.

Past studies have shown that the ebb-delta/inlet influence on beaches either immediately behind the ebb delta or adjacent to it is exerted through various processes. These include wave sheltering by the ebb tidal body (FITZGERALD *et al.*, 1979), wave refraction effects which can cause littoral drift to be locally trapped on the downdrift side of the ebb delta (HAYES and KANA, 1976), littoral drift bypassing effects, and temporary or permanent trapping of beach sand on the deltas (FITZGERALD and HAYES, 1980; FITZGERALD, 1984). Most of this work has been focused on descriptions and conceptual models for the various processes involved.

Characteristic time and spatial scales of change associated with various processes have been reported. The work of FITZGERALD and associates on mixed energy shores (*e.g.*, FITZGERALD and HAYES, 1980; FITZGERALD, 1988) has shown 3-10 year erosion and accretion cycles associated with the growth of sand bar complexes on the ebb delta platform, the shoreward migration of these bars, and their eventual welding onto the adjacent beach. Irrespective of whether the inlet bypasses significant volumes of sand alongshore or simply circulates sand around the ebb-delta/inlet system in a closed

loop, this sand transfer occurs mainly in packets, with sand accretion on the adjacent beach and/or releases alongshore being limited by the rate at which bar complexes can migrate landward off the ebb delta. The time scale of these cycles tends to be shorter at smaller inlets, which have smaller ebb deltas (WALTON and ADAMS, 1976; HICKS and HUME, 1996). Similarly, the length of shore affected increases as the ebb delta size increases. The migrating bars also extend further alongshore when the main ebb channel is inclined at a lower angle to the gross shoreline trend. Migrating bar complexes ranging in length from 300 m to several km and inducing shoreline erosion/accretion shifts of tens to over 100 m have been described (*e.g.*, FITZGERALD and NUMMEDAL, 1983; FITZGERALD, 1984; SMITH and FITZGERALD, 1994). Larger scale shore erosion/accretion cycles spanning periods of 7–40 years occur also. These are governed by the orientation of the main ebb channel, which cyclically flips to either side of the shore-normal. Shoreline shifts of 300–400 m and extending several km alongshore have resulted (*e.g.*, FITZGERALD, 1984).

Most recently, FENSTER and DOLAN (1996) determined, by examining the rate of change of shoreline position over a 40 year time span, that on mixed-energy, tide-dominated coasts inlet effects dominated shoreline change within 4.3 km of the inlet and influenced the coast for up to 6.8 km on the updrift side of the inlet and 5.4 km on the downdrift side. On wave dominated coasts they found that the scale of dominance was the same, but that the total span of influence extended up to 13 km on the downdrift side of the inlet.

A key finding from this past work is that tidal delta-inlet systems disrupt the longshore continuity of the littoral drift stream by bypassing sand in discontinuous packets. Thus when the ebb delta is accumulating sand, which may occur over several years, the downdrift shore must erode to make up the sand supply deficit and an erosion 'wave' may be initiated. When the delta releases sand, as when bars weld to the shore, a migrating sand 'slug' is initiated (*e.g.*, BRUUN, 1954; DOLAN, 1970). Such perturbations potentially induce erosion/accretion cycles well alongshore from the inlet but, because they probably occur over multi-year time scales and their magnitudes attenuate alongshore, they may be difficult to detect against the larger amplitude, more frequent storm-induced changes that characterise beaches far from the inlet.

In this paper, we investigate patterns of beach change over a four year period along 25 km of shore centred on a natural, mixed-energy, tide-dominated inlet with a large ebb delta. Our aims are to isolate the magnitudes, spatial patterns, characteristic time scales, and causes of the main erosion and accretion signals, both within the shadow of the ebb delta and further alongshore. A companion paper (HUME *et al.*, in preparation) describes the morphodynamics of the ebb delta in greater detail.

PHYSICAL SETTING

Katikati Inlet is located in the western Bay of Plenty on New Zealand's North Island (Figure 1). It forms the northern entrance to Tauranga Harbour, a large (~ 200 km²) meso-tidal estuarine lagoon which is separated from the sea by the

24 km long mainly Holocene sand barrier of Matakana Island (MUNRO, 1994). The 80 km² of the lagoon that Katikati inlet drains has extensive intertidal areas. The spring tidal prism is 95×10^6 m³ and is dominated by tidal flows (HICKS and HUME, 1996). It is a natural inlet, without artificial structures, dredging, or sand extraction. A rock headland on the northern shore provides positional stability to the inlet, a situation typical of tidal inlets on this part of the New Zealand coast (HUME and HERDENDORF, 1992). The inlet has only a small active flood-tide delta capping an older shoal (DAVIS *et al.*, in preparation). The ebb tidal delta is an order of magnitude larger, extending offshore for about 3 km to 20 m depth, spanning 6 km alongshore, and storing some 30×10^6 m³ of sand (HICKS and HUME, 1996).

Morphologically, the Katikati ebb delta consists of a triangular-shaped, largely subtidal swash platform, offset slightly to the south-east of the inlet (Figure 2). The main ebb tidal channel crosses this platform, first at a southerly inclined angle to the general shore-normal direction because of the rock controls on the ebb jet through the inlet throat, then it re-curves northward to be more shore-normal towards the outer margin of the delta. The inner channel has well defined linear bars along its margin, while the outer channel terminates in a depositional lobe. Marginal flood-tide channels feed into the inlet from both sides between the delta platform and the adjacent shore. Wave-built linear bars front the northern side of the platform, merging near the shore with bars that are sub-parallel to Waihi Beach. On the south-east side of the platform, linear bars lie sub-parallel to the inlet shore, while the platform front often contains large transitory arcuate bars. These linear and arcuate bars periodically weld onto the cusped foreland that marks the southern entrance to the inlet. The morphodynamics of the ebb delta and sand transport pathways are detailed by HUME *et al.* (in preparation). The delta is composed of fine sand, slightly finer in texture and similar in composition to that on the adjacent beaches.

Waihi Beach, on the north-west side of the inlet, extends 8 km between the Katikati headland and the beginning of a rocky cliffed shore at Waihi. Historically, its average shoreline position appears to have changed little since the first cadastral plans were surveyed in 1870 (R.K. SMITH, personal communication; GIBB, 1994), although short-term shoreline fluctuations up to 70 m wide have been observed (HARRAY, 1976). It comprises fine to medium sand but with the sand close to the ebb delta being noticeably coarser than elsewhere on the beach.

Matakana Island, the barrier island on the south-east side of the inlet, has a notable cusped foreland or 'humpback' opposite the south-eastern margin of the ebb delta, resulting in the 'drumstick' plan view that is typical of barrier inlet systems (HAYES and KANA, 1976). Historically, the Matakana Island open-coast shoreline has experienced short-term fluctuations of 20–30 m but little net change (GIBB, 1994). Close to the inlet, between the humpback and the inlet throat, the Matakana shore has experienced severe spates of erosion and accretion, with migrations up to 300 m over periods of 3–5 years.

In the western Bay of Plenty, the astronomical tides are

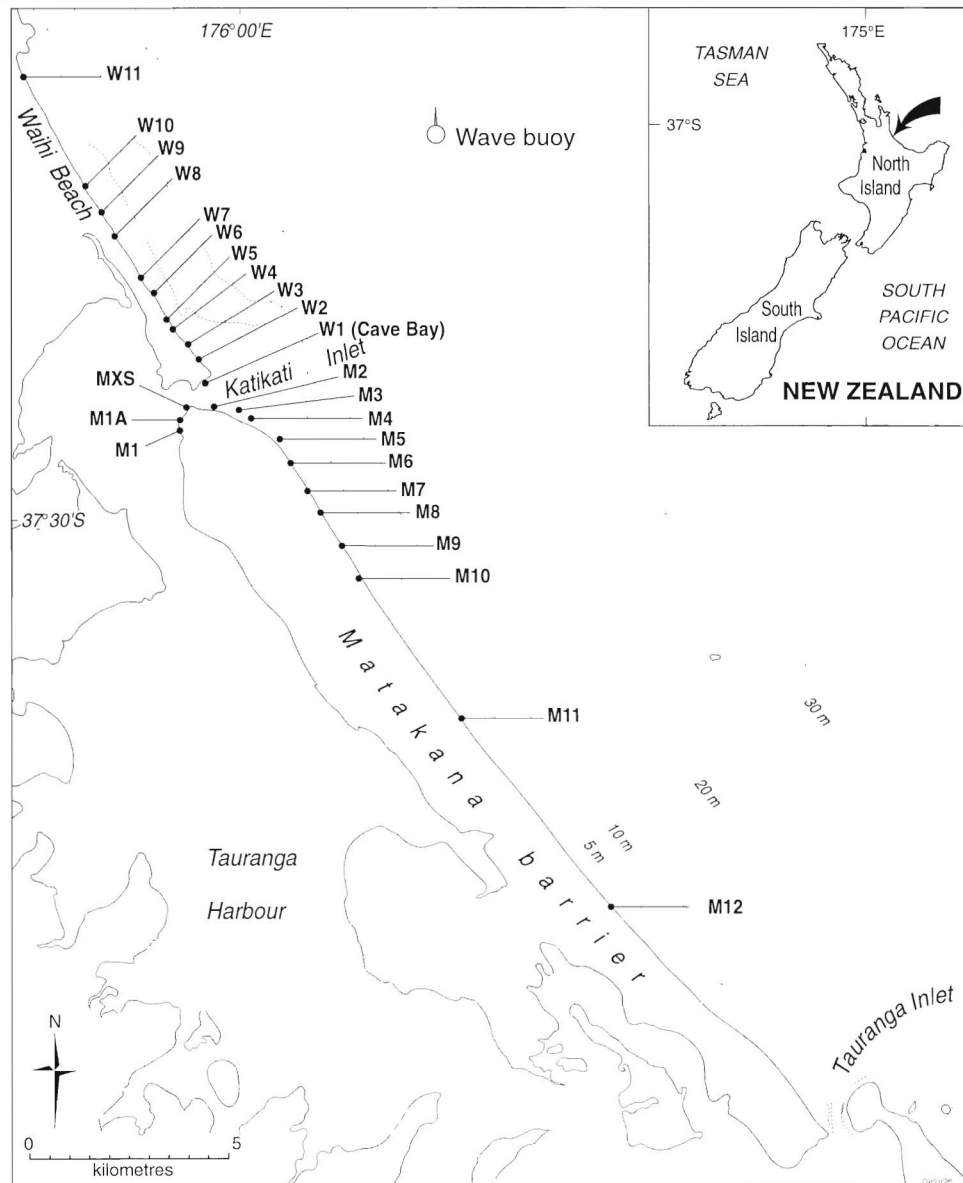


Figure 1. Map showing Katikati Inlet and ebb tidal delta, Waihi and Matakana Island Beaches, beach profiles (W and M numbers), nearshore bathymetry, and wave buoy location.

semidiurnal and the mean neap and mean spring tidal ranges for the open coast are 1.26 and 1.64 m respectively. Sea-level set-ups associated with storm surges range up to 700 mm, while the barometric effect causes local sea level to change by between -4 and -10 mm.hPa $^{-1}$ (BELL and GORING, 1996).

Nearshore currents (5–10 m water depth) on the open coast are dominantly shore parallel, with speeds ranging from 0–0.30 ms $^{-1}$ and a median speed of around 0.05–0.07 ms $^{-1}$ (WILLIAMS and BELL, 1991; HUME *et al.*, in preparation). The tidal constituents account for about 25% of the variation in the current records in the longshore direction. Significant wave heights over the four year study period were less than

1 m for 70% of the time, averaging 0.8 m and peaking at 4.7 m (MACKY *et al.*, 1995). Significant wave periods averaged 6 seconds, while most of the wave energy was found at periods between 7 and 13 seconds and arrived from the northeast-easterly sector, which straddles the regional shore-normal direction. The long-term net littoral drift on the Bay of Plenty coast appears to be generally towards the southeast but, at least in the western part of the Bay, is small compared to the gross drift (EWART, 1961; GIBB, 1977; HARRAY and HEALEY, 1978; MACKY *et al.*, 1995).

The wave and tidal regime at Katikati Inlet classifies the inlet as “mixed energy, tide-dominated” (HAYES, 1979; NUMMEDAL and FISCHER, 1978). The ebb delta also rates a “mixed

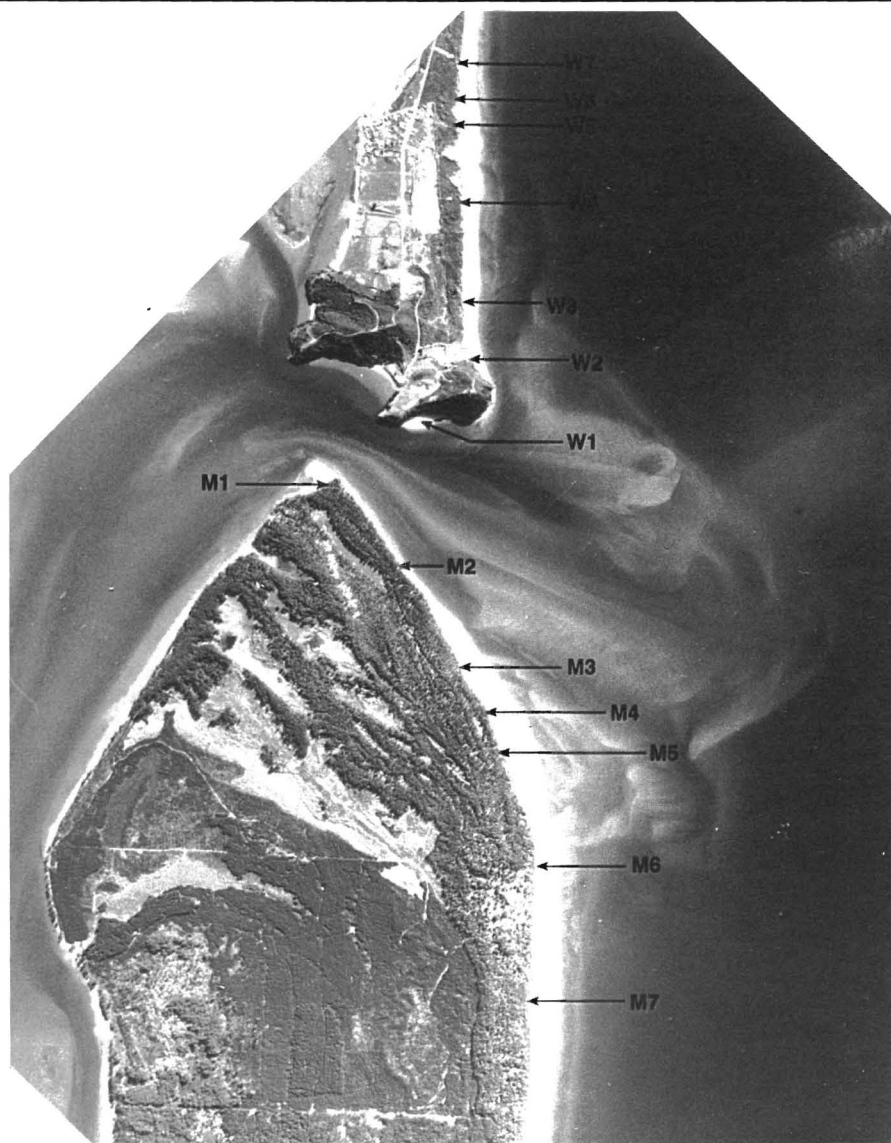


Figure 2. Aerial photograph (1988) of the ebb tidal delta and adjacent beaches, showing the morphological features on the ebb delta and the near field profile locations.

energy, Group 2" classification in the scheme of GIBEAUT and DAVIS (1993), owing to its arcuate shape, the asymmetry induced by the orientation of the main ebb channel, and the well-developed landward migrating swash bars on the ebb delta platform. The ratio of net annual littoral drift to spring peak tidal discharge is approximately equal to 12 (HUME *et al.*, in preparation), which suggests, from the scheme of BRUUN (1990), that tidal processes are likely to be the main means of bypassing and transferring sand around the ebb delta.

METHODS

General Approach

The study included five tasks: (i) monitoring a network of profiles along the beaches adjacent to and behind the ebb

delta; (ii) extracting patterns of shoreline and sand volume change from the profile dataset, including identifying the longshore extent of the inlet effects; (iii) monitoring waves and sea level; (iv) correlating these forcing functions with the shore change in order to identify the main processes driving the shore change; and (v) matching these processes with morphological evidence on and around the ebb delta.

Beach Profile Surveys and Analysis

In October 1990, 25 beach profiles were established along the 25 km span of the study shore (Figure 1). The profile spacing increased away from the inlet. All profiles were re-surveyed at approximately monthly intervals from August 1991 until January 1995. The survey method was a variant

of EMERY'S (1961) technique, with two 1.6 m poles used to measure height differences and a tape to measure distances. The surveys, conducted about the low tide, extended from the dunes (up to 7.8 m above mean sea level) to below low tide level (down to 1.2 m below mean sea level). In December 1991, the survey of these beach profiles was combined with a detailed bathymetric survey of the ebb delta and the near-shore region off the adjacent beaches (HICKS and HUME, 1997).

The analysis of the beach profile dataset was based on two parameters: the sand volume (V) above the MSL datum and the excursion distance (X) from the landward end of the profile to the MSL contour. These parameters were normalised (to V^* and X^*) by taking the deviation from the mean values for each profile over the study period. Thus X_{ij}^* , for survey i of profile j , was the gain or loss in sand volume above MSL from the average volume at profile j . V^* was found to be highly correlated with X^* , and so most of the subsequent analysis focused on explaining the V^* signal.

Excluding the three profiles in the inlet throat, the spatial and temporal patterns shown by V^* and/or X^* were extracted from: (i) the range and variance over the study period at each site; (ii) the time trends in V^* accumulated along several sub-reaches of the study shore; (iii) dispersion diagrams; and (iv) principal components analysis.

Four sub-reaches of the open-sea-facing shore were defined, representing the 'near field' (in the 'lee' of the ebb delta) and 'far field' areas of influence of the ebb delta on both sides of the inlet. Their boundaries were fine-tuned from the longshore pattern of V^* and X^* . Net sand volume changes in each sub-reach and along the whole shore were determined from the changes at the component profiles by integrating the average change between adjacent profiles multiplied by their separation distance.

'Dispersion diagrams' are useful for visually identifying temporal and longshore signals in sand volume or other parameters (e.g., HASHIMOTO and UDA, 1982; HICKS and INMAN, 1987). They are particularly good for identifying sand wave migrations, which show up as diagonal trends (hence the term 'dispersion diagram'). In this study, dispersion diagrams were prepared using grids of V^* and X^* constructed at intervals of 500 m alongshore and 14 days in time using a linearly-interpolating triangulation algorithm with a $\times 20$ weighting assigned to the time values to correct for the anisotropy induced by the different time and distance scales (GOLDEN SOFTWARE, 1994). Similar dispersion diagrams were also prepared for the rate-of-change of volume and MSL excursion distance, dV/dt and dX/dt , respectively. It was hypothesised that these latter diagrams would better depict the signature of discrete events (such as coastal storms and accretion phases) while the X^* and V^* diagrams would better depict cumulative trends.

Principal components analysis (PCA), which resolves the variance structure of a multi-variate data set, is commonly used to interpret records of cross-shore or longshore beach change (e.g., WINANT *et al.*, 1975; AUBREY, 1979; DOLAN *et al.*, 1982; HASHIMOTO and UDA, 1982; MEDINA *et al.*, 1991). The approach isolates characteristic, independent modes of covariance or correlation (normalised covariance) among the

original variables. When used to identify longshore patterns, each mode has a characteristic 'loading' at each site alongshore and a varying 'score' with time. Since the first few principal components typically account for 90% or more of the variance in the original dataset, the technique tends to be very effective at condensing the original data into a few plots. PCA was applied to the beach volume (V^*) dataset using the software package STATISTICA (STATSOFT, 1991). The analyses were conducted for the whole span of shore and for the four sub-reaches described previously. Cross-correlation analysis was used to establish how each principal component score related to the records of waves and sea level.

While there is some redundancy in the results from techniques (i)–(iv), they are mutually supportive since one method may provide a ready explanation for features in another. They all, however, offer unique results. For example, the simple statistics of X^* convey the most information on the magnitudes of shoreline change, the trends in V^* within sub-reaches provide sand budget information, the dispersion diagrams highlight wave-like morphological features, while PCA is the only technique which shows the proportion of the total shoreline variance associated with individual processes.

Waves and Sea level: The Forcing Functions

Directional wave data were recorded over 17 minutes at 3-hour intervals for a period of four years by an ENDECO buoy located 8 km seaward of the ebb delta in 34 m water depth (MACKY *et al.*, 1995). These data were used to compute a record of the dimensionless 'fall speed' parameter, H_{s0}/wT (where H_{s0} is the significant wave height in deep water, T is the wave period, and w is the beach-sand fall speed), which we used as an indicator of whether the shore should have been generally eroding or accreting. Essentially, this parameter compares the height to which waves disperse sand above the bed with the distance the sand can fall back down during a wave period. Net sand transport is expected to be onshore when this ratio is low, due to the asymmetry of shoaling waves, and offshore when the ratio is high and waves steeper (DEAN, 1973). Laboratory and field studies of beach erosion/accretion under irregular wave conditions (see LARSEN and KRAUS, 1989, for a review) suggest empirically that beaches should accrete when $H_{s0}/wT < 3.2$ and they should erode when $H_{s0}/wT > 3.2$ (where it is assumed that for a Rayleigh distribution of wave heights, H_{s0} equals 1.6 times the mean wave height).

This empirical criterion is based on the assumption that the existing beach profile is reasonably close to an equilibrium condition (LARSEN and KRAUS, 1989). Nevertheless, a time series of H_{s0}/wT is a useful qualitative index of whether the beaches should have been eroding or accreting over the study period. A representative fall speed was taken as 0.036 ms^{-1} based on a median (d_{50}) sand size of 0.28 mm (HICKS and HUME, 1996) and equation 4–8 of CERC (1984). When the wind was offshore and the representative wave condition at the buoy was offshore (*i.e.*, when there were no waves at the shore), H_{s0}/wT was assigned a value of 3.1, which is the average value for all onshore waves recorded over the 4 years. This value was assumed to represent conditions when the

beach was neither accreting or eroding due to cross-shore transport, and is very close to the 'neutral' value of 3.2 presented by LARSEN and KRAUS (1989).

Regional longshore transport was estimated assuming a shore with straight and parallel contours trending 31° West of North and applying linear wave theory and Snell's law to shoal and refract the wave conditions measured at the buoy shoreward to the breaker zone. The resulting time-series of breaking wave conditions was combined with the CERC (1984) 'wave energy flux factor' equation to compute the potential longshore transport. The longshore transport rate (Q_1 , in $m^3 d^{-1}$) is

$$Q_1 = 9596 H_{sb}^{2.5} \sin 2\alpha_b \quad (1)$$

where H_{sb} is the significant breaker height and α_b is the breaker angle.

A more detailed refraction-diffraction study was carried out to identify the changes in the wave field due to local-scale bathymetric features, notably the ebb delta, and the consequent effects on the rates and longshore gradients of longshore transport. This employed a variation of the numerical wave refraction model RCPWAVE (EBERSOLE, *et al.*, 1986; GREEN, 1994) to predict the breaking wave conditions at each of the ocean-facing beach profile sites. To cover much of the observed deep water wave climate, waves of 2.0 m significant wave height with periods ranging from 4.5 s to 10.5 s and source directions ranging from 15° east of north to 95° east of north were processed. The rectangular bathymetry-grid used for the refraction model was generated from the 1991 bathymetric and beach survey datasets (HICKS and HUME, 1997). Wave energy dissipation was ignored in the refraction model runs.

The potential longshore transport rate at each beach profile site was estimated using the equation of HANSON and KRAUS (1989):

$$Q_1 = (H_s^2 c_g)_b \left[a_1 \sin 2\alpha - a_2 \cos \alpha \frac{\partial H_s}{\partial x} \right]_b \quad (2)$$

where H_s is the significant wave height, the subscript b denotes breaker conditions, α is the breaker angle with respect to the nearshore contours at the break-point, and c_g is the wave group speed (estimated as $(gH_s)^{0.5}$). a_1 and a_2 are dimensionless parameters defined by

$$a_1 = \frac{K_1}{16(\rho_s/\rho - 1)(1 - p)(1.416)^{2.5}} \quad (3)$$

$$a_2 = \frac{K_2}{8(\rho_s/\rho - 1)(1 - p)\tan \beta (1.416)^{3.5}}$$

where ρ_s/ρ is the density ratio of sand and water (taken as 2.65), p is the porosity of sand on the seabed (taken as 0.4), K_1 and K_2 are empirical efficiency parameters for the transport that is driven by obliquely incident waves and the longshore gradient in wave height, respectively, $\tan \beta$ is the average slope across the longshore transport zone, and the factors involving 1.416 are to convert from significant wave height to root-mean-square wave height. K_1 was taken to be 0.77, as originally determined by KOMAR and INMAN (1970). K_2 was assumed to be 0.38, equal to half of K_1 as is often

assumed as a starting point with numerical shoreline modelling (*e.g.* GRAVENS *et al.*, 1991). $\tan \beta$ was estimated from empirical relationships given by HANSON and KRAUS (1989) which relate $\tan \beta$ to the deep-water wave height and steepness and the median beach sand size. Equation (2) includes a term for the effect of a longshore gradient in wave height. This term may become significant where the nearshore topography changes sharply, as around an ebb delta, or where bathymetric irregularities induce wave focusing.

The longshore gradient in longshore transport was determined by differencing the transport rate between adjacent beach profile sites. The divergence patterns generated were used to identify the wave conditions when longshore transport was stalled by the ebb delta, and to help explain the longshore loadings of the principal components.

A permanent open-coast sea-level recording station, located 25 km south-east from Katikati Inlet at Moturiki Island off Tauranga Inlet (Figure 1), provided a 15-minute digital record of sea level through the study period (GORING and BELL, 1996). A 28-day running-mean sea level was extracted from this record for comparison with the beach changes.

Ebb Delta and Shore Morphology

The morphology of the study shore and the shallower parts of the ebb tidal delta were monitored over the study period through a combination of ground and air photographs and visual observations. The migrations of bars, erosion 'holes', and tidal channels were traced to derive a conceptual appreciation of the processes responsible for sand gains and losses.

RESULTS

Morphologic Change

The observed changes in morphology on the far field beaches over the study period were typical of open-coast beaches responding to wave events. A small progressive sand loss was observed on Matakana Island. More noticeable changes occurred on the near field beaches. Within the inlet throat, Cave Bay and the tip of Matakana Island spit (sites W1 and M1 on Figure 2) tended to accrete in unison at the same time as the nearby ocean-facing beaches (W2 and M2) eroded. This change was observed after periods of high energy easterly waves. We infer that these waves swept sand into the inlet, some of it being caught on the throat beaches and some being injected into the main tidal channel.

At the eastern, near field end of Waihi Beach (profiles W2-W5 on Figure 2), an erosion trough was seen to migrate westward during the study period while an accretionary pulse began at W2 in 1994. The trough related mainly to the position of the western marginal flood tide channel, which was forced to move by a sand bar migrating shoreward from off the western margin of the ebb delta. Accretion followed when the flood channel jumped seaward and the bar welded to the beach. The erosion trough was also affected for a time by wave focusing through a gap in the offshore bars (Figure 3). In similar fashion, a trough migrating along the Matakana near field beach (profiles M5-M2), followed by accretion, related to the scouring action of the eastern flood channel,

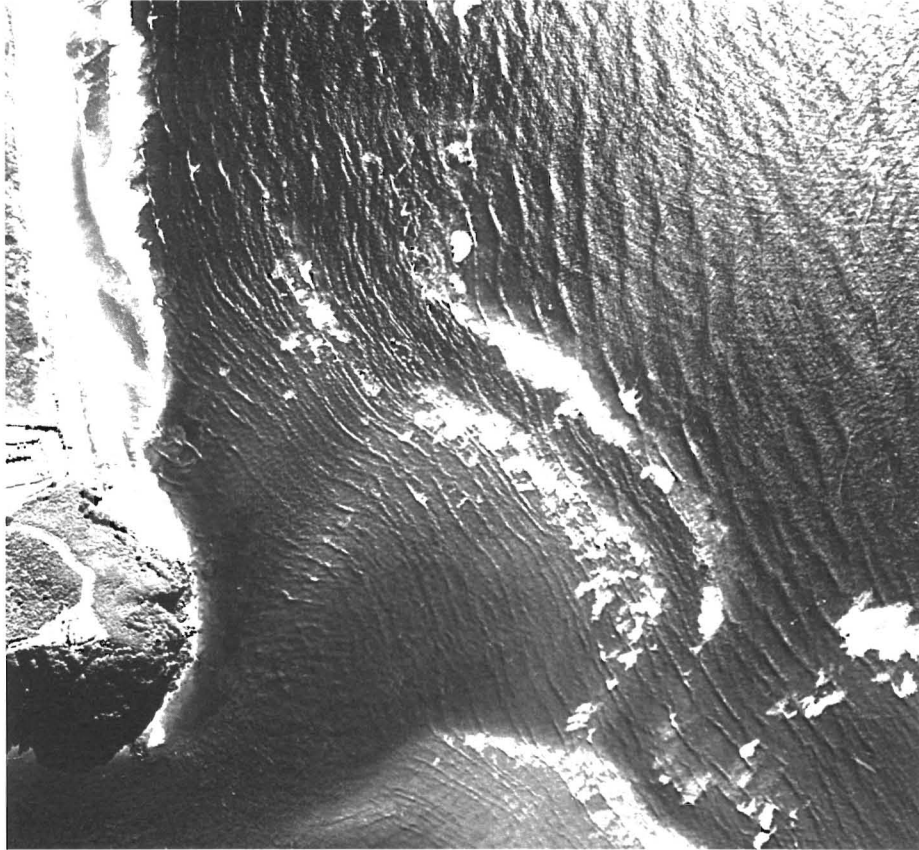


Figure 3. Erosion hole on Waihi shore between W2 and W3 showing wave focusing through a gap in the inner offshore bar (13 July 1991).

which was forced against this shore for a time by sand bars migrating shoreward from the eastern ebb delta platform (Figure 4). The accretion phase began when the bars welded onto the cusped foreland (at M5).

Morphologic changes on the Katikati ebb delta through the study period are detailed in a companion paper (HUME *et al.*, in preparation).

Waves and Sea level: Patterns and Correlations Among the Forcing Functions

Time-series of wave height, fall speed parameter, potential longshore transport rate, and accumulated net potential longshore transport are plotted in Figure 5 along with the 28-day mean sea-level record. Figure 5a shows no clear regularity or seasonality in the occurrence of storm waves, although storms often occurred in spates with extended relatively calm periods between (*e.g.*, September 1991 to June 1992). The fall speed parameter plot (Figure 5b) suggests episodes of erosion (H_{so}/wT highs—corresponding to steep storm waves) and longer periods of accretion (H_{so}/wT lows—corresponding to swell).

Figure 5c shows that the longshore transport potential varied considerably in magnitude and direction, even from day to day, with ‘instantaneous’ rates sometimes exceeding $100,000 \text{ m}^3 \text{ d}^{-1}$ (*e.g.*, on 23 October 1992, when the wave con-

ditions recorded at the wave buoy were $H_s = 3.9 \text{ m}$, $T = 7.4 \text{ s}$, and the angle of approach to the regional shoreline trend was 25°). This ‘flip-flop’ pattern is primarily related to changes in the direction of waves, most of which approach very nearly normal to the shore. Systematic periods of net drift only become apparent in the record of accumulated longshore transport (Figure 5d). This shows something like a three-year cycle in the net drift, with an extended phase of net easterly drift (albeit with some temporary reversals) from May 1991 to October 1992, then generally westward transport until May 1994, then generally eastward transport again. While the net calculated drift rate over the 4 year study period was $57,000 \text{ m}^3 \text{ y}^{-1}$ to the west, it is clear from Figure 5d that this average figure is very dependent on the time span (*e.g.*, our figure differs from the $70,000 \text{ m}^3 \text{ y}^{-1}$ reported by MACKY *et al.*, 1995, whose calculation used the same formulae but only the first 3 years of the wave record). For another period, the average could well be in the reverse direction.

Further caution should be attached to the estimate of average net drift rate due to its sensitivity to systematic errors in the breaker angle. An error of a few degrees is possible in this from the compass setting on the wave buoy and/or in defining the regionally representative shoreline orientation. While such errors induce minor uncertainty on the gross

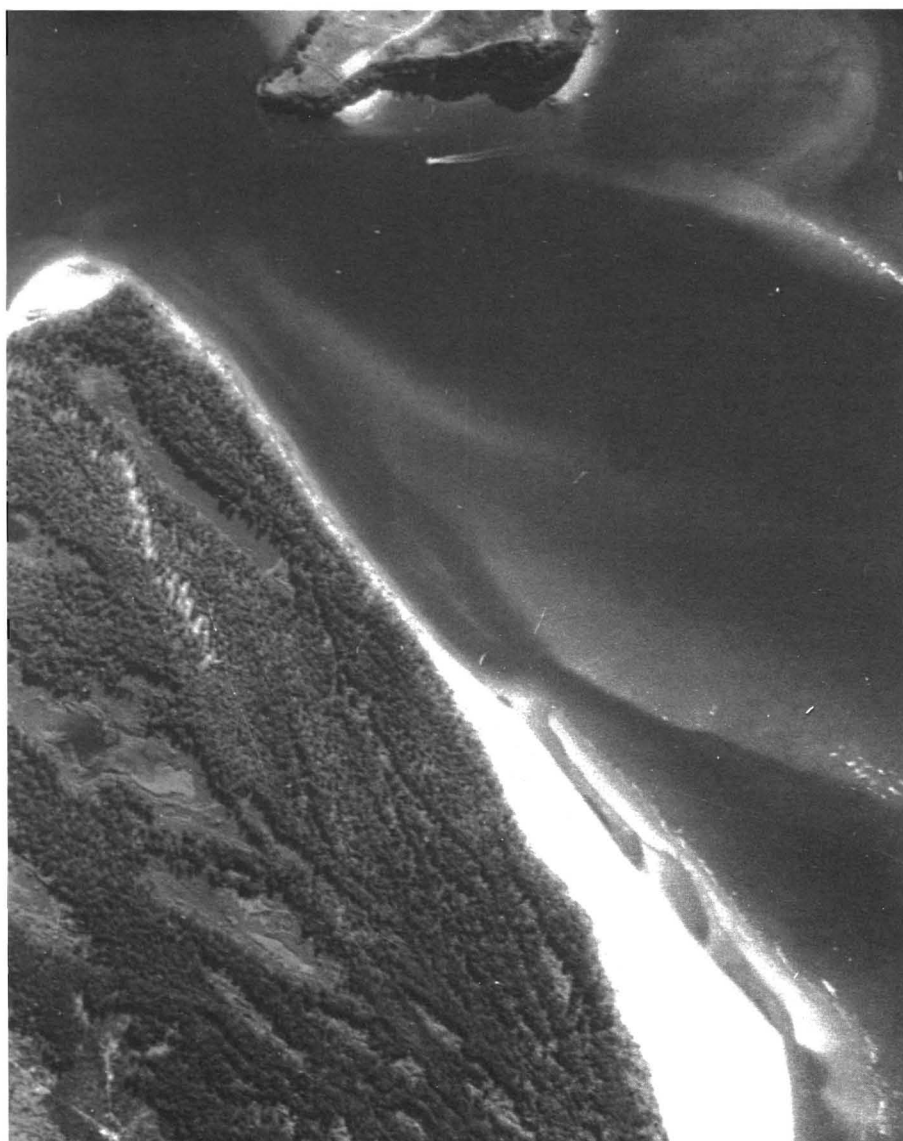


Figure 4. Erosion embayment cut in the Matakana shore by the flood tide marginal channel which is directed at the shore by bars on the delta platform.

drift, the average net drift is a classic example of a small number with large uncertainty obtained by differencing large numbers with small uncertainty (*i.e.*, the total drift to east and west). A sensitivity analysis, which involved systematically changing the breaker angle by $\pm 1^\circ$, 2° , and 5° , induced respective changes of only approximately $\pm 1\%$, 2% , and 5% in the average gross drift ($1,290,000 \text{ m}^3\text{y}^{-1}$) but $\pm 70\%$, 140% , and 350% in the average net drift ($57,000 \text{ m}^3\text{y}^{-1}$ west). Thus we conclude that over the four year record period the gross drift was large relative to the net drift, and any net drift was of indeterminate direction. The sensitivity analysis showed, however, that the inter-annual pattern of net drift reversal, as described above, was not significantly influenced by systematic changes in the breaker angle—the 3-year cycle still

occurred, albeit with episodes of more intense transport in the direction to which the bias was applied.

The 28-day average sea level (Figure 5e) varied over a range of 0.2 m through the study period. While this range was small relative to the spring tidal range (1.65 m), the sea-level anomalies lasted typically of the order of 6 months, which should be an adequate period to initiate some degree of 'Bruun-rule' type shoreline adjustment (BRUUN, 1962).

Auto- and cross-correlation analyses were conducted on these forcing-function parameters to quantify any regularities and inter-connections in the signals shown in Figure 5. Unless specified otherwise, the level of statistical significance for the correlation coefficient, r , was set at 5%. The auto-correlation results showed weak but significant annual cycles

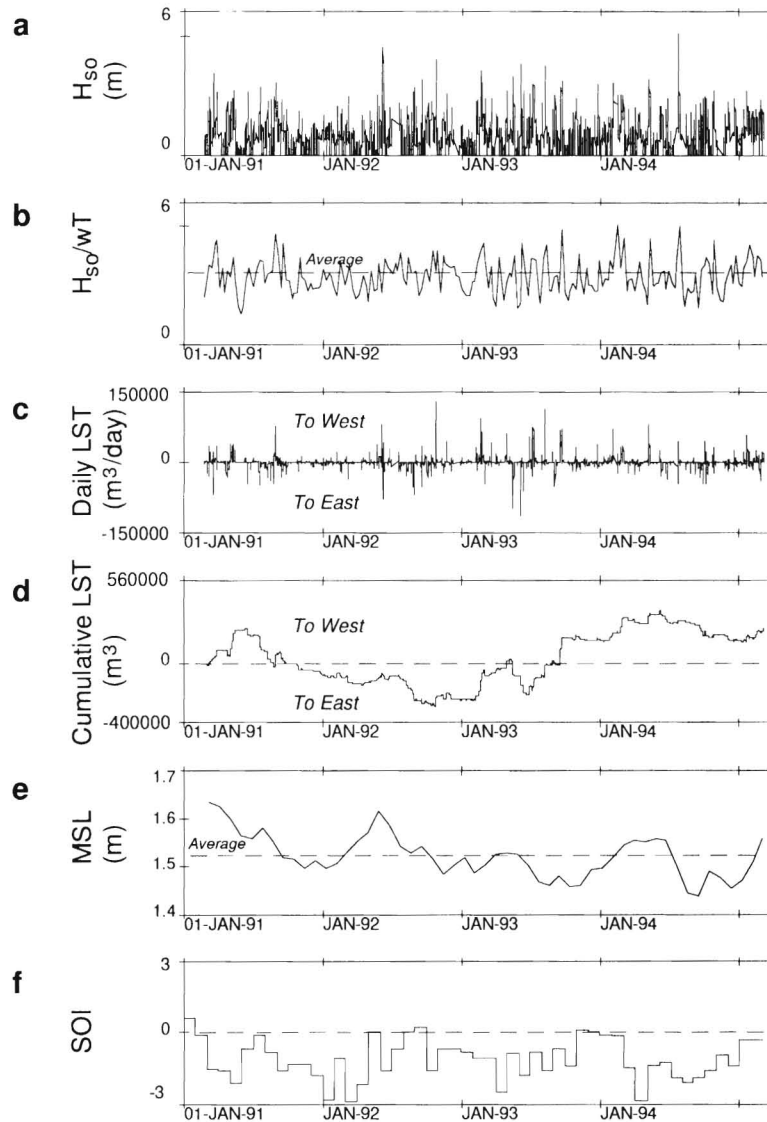


Figure 5. Time series plots of: (a) Deep-water significant wave height, (b) Fall speed parameter (7-day average), (c) Daily longshore transport potential (positive transport is to the west), (d) Cumulative (*i.e.*, net) longshore transport since the beginning of the wave record, (e) Mean sea level (28-day average), and (f) Southern Oscillation Index (monthly average).

both in sea level (a seasonal sea-level signal in the Bay of Plenty was also identified by BELL and GORING (1996)) and the fall speed parameter. Sea level tends to be higher during the autumn equinox, while the fall speed parameter tends to be higher in the late winter–spring and lower in summer–autumn. The maximum cross-correlation between sea level and fall speed parameter ($r = 0.57$) was achieved with a lag of 6–7 months. Thus, on a seasonal basis, the fall speed parameter (which is essentially an index of the beach erosion potential of the incident waves) tends to be higher when the mean sea level is lower—a fortuitous combination for beach stability along the study shore. Mean sea level in the Bay of Plenty is well correlated with the Southern Oscillation Index (SOI—Figure 5f) at a quasi 4-year inter-annual time scale,

with sea level lagging the SOI by some 9 months and being low when the Southern Oscillation is in its negative, El Niño, phase (BELL and GORING, 1996). There is an indication also of correlation of both sea level and fall speed parameter with the SOI for monthly fluctuations (compare Figures 5b and 5e with 5f), with the fall speed parameter showing a significant correlation with the SOI ($r = -0.56$) at a lag of 4 months.

No seasonal signal is evident in the potential longshore transport signal. However it is possible that the quasi 3-year cycle suggested in Figure 5d is associated with an inter-annual mechanism such as the Southern Oscillation. There is an inverse correlation ($r = -0.31$; significant at 6% level) between the SOI and net longshore transport at monthly scales, with transport tending north–westward when the SOI is

more negative (*i.e.*, towards El Niño conditions, when south-easterly-westerly weather is more prevalent in the mid-latitudes) and south-eastward when the SOI tends more positive (*i.e.*, towards La Niña conditions, when north-easterly weather is more common). It should be borne in mind that through much of the four-year study period the SOI was negative (Figure 5f), with the Southern Oscillation in its El Niño mode.

Littoral Drift Divergence

The effects of wave refraction on the longshore gradient in longshore transport (Figure 6) indicate that the significant effects of the delta extend between profiles W9 and M9. Outside this zone, the predicted transport rates vary relatively little alongshore. Within this zone, the influence of the ebb delta varies according to the period and direction of the incident waves. Waves with periods up to 8.5 seconds tend to result in a consistent longshore transport pattern, with the refraction becoming greater, and the longshore transport divergence consequently becoming greater, as the period increases. Longer period waves divert from this pattern; apparently, their longer wavelengths are more strongly influenced by the ebb delta morphology. Transport direction reversals are common on the eastern, Matakana side of the inlet but are rare on the western side. For incident waves arriving from 55° East of North, which is essentially normal to the regional shoreline trend, the far field transport rates are close to zero while in the near field the refraction-modified transport rates are much higher and are directed towards the inlet from both sides (Figure 6b).

For a given wave period, the amplitude of the longshore gradients in longshore transport and the asymmetry about the inlet both increase as the incident wave travelling direction rotates clockwise (Figure 6d). For example, 8.5 s waves from 15° East of North induce relatively little change from the far field transport rate on the western wing of the ebb delta and have a slightly greater effect on the eastern wing. When the waves are normally incident, arriving from 55°, the effect is greater on both sides but more on the eastern side.

While the actual longshore transport rates and directions vary considerably as the incident wave direction changes (Figure 6d), their longshore gradients, or divergences, maintain a remarkably consistent pattern (Figure 6e). This indicates that irrespective of whether the regional longshore transport is to the west, east, or the waves are normal to the shore, longshore transport should cause erosion on the ebb delta margins, accretion closer towards the inlet, and relatively little change on the far field beaches. When the transport is eastward (*e.g.*, direction = 15° on Figure 6d) the delta margin erosion is associated with a local acceleration in the eastward transport; when the waves arrive normally (*e.g.*, direction = 55°) a local transport system is set up that drives sand towards the inlet from both sides; and when the transport is westward (*e.g.*, direction = 95°) the delta margin erosion is associated with a local acceleration in the westward transport.

Obviously, such a consistent longshore transport divergence pattern for all wave directions cannot persist without shoreline perturbations growing unless other processes act to

renourish the delta margin erosion zones and to scour the deposition zones closer toward the inlet. Later discussion suggests that these processes are landward migrating sand bars and scouring flood-tidal flows, respectively.

Beach Profile Volumes and Excursion Distances

Variance and Near- and Far Field Definitions

The range and variance of the mean sea level excursion distances and beach volumes for the ocean-facing profile sites (Figure 7) show highest variation, particularly in beach volume, in the lee of the ebb delta, between profiles W4 and M5 (V^* changes up to 275 m³m⁻¹ and X^* changes up to 165 m). In comparison, in the far field the beach changes were more uniform and smaller (V^* up to 70 m³m⁻¹ and X^* up to 50 m). W4 marks the westward extent of major sand bars on the Waihi side of the ebb delta (Figure 2). M5 marks the apex of the cusped foreland on the Matakana side of the delta, where sand bars migrating shoreward from the delta tend to attach to the beach. However, the nearshore morphology suggests that distinctive inlet-related sand bar activity extends almost as far west as W5 and as far east as M7 (Figure 2), 2 km and 3 km from the inlet centre-line, respectively. Thus from the combined evidence of the beach variance and the nearshore morphology, for the purposes of the analyses of beach volumes and principal components we re-defined the near field of the inlet-delta influence as lying between W5 and M7.

The Pearson correlation coefficients between beach volume, V^* , and excursion distance, X^* , at each profile ranged from 0.41 to 0.97, averaging 0.74. All of these correlation coefficients were significant at the 5% level, thus confirming that analysis could be concentrated on one parameter or the other.

Beach Volumes

Unit beach sand volumes (m³m⁻¹) were determined for four sub-reaches spanning the ocean-facing shore: Waihi far field (W11-W6); Waihi near field (W5-W2); Matakana near field (M2-M7); and Matakana far field (M8-M12). The average unit volume for the entire shore (Figure 8a) showed a quasi-seasonal pattern of sand gains and losses superimposed on a trend of net sand loss. Sand gains tended to occur in the early summer and losses in the winter. The volume changes in the separate sub-reaches (Figure 8b) showed firstly that the short-term fluctuations in volume were in-phase alongshore, and secondly that the net overall sand loss was due to sand losses in the near field sub-reaches, notably on the Matakana shore. In contrast, the far field sub-reaches experienced little net sand volume change. The sand losses from the near field beaches are expected to be matched by sand gains on the ebb delta and inside the inlet. Certainly, the beach volumes at Cave Bay on the western shore of the inlet throat (W1) and on the inside of the Matakana spit (M1) tended to increase when the nearby ocean-facing beaches (W2 and M2) eroded (Figure 8c).

Significant correlations were found between the fall speed parameter (Figure 5b) and sand volume for the whole shore and for the two far field compartments, indicating the direct

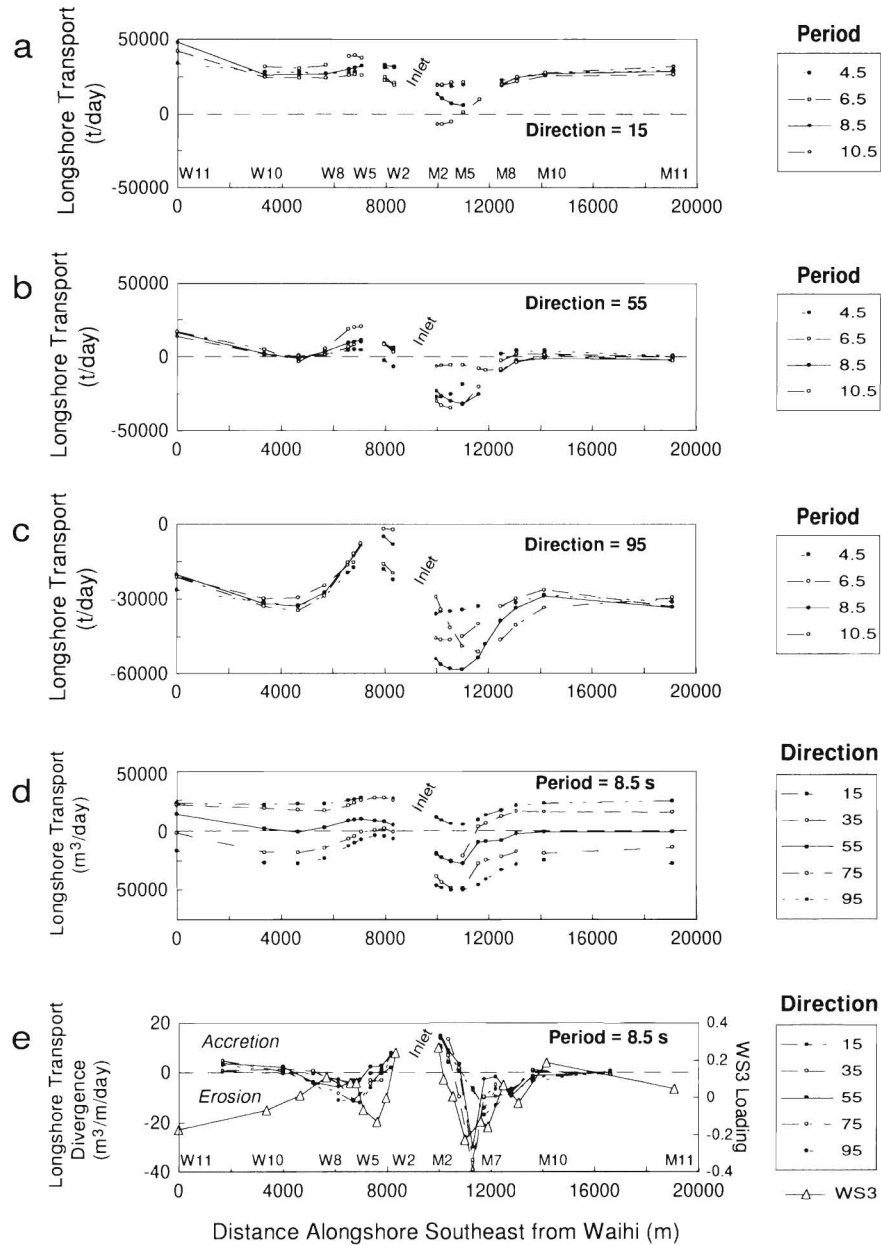


Figure 6. Longshore variation in potential longshore transport rate and divergence for varying wave directions and periods, computed at the open-ocean-facing profile locations. Katikati Inlet is located approximately 9,000 m from the distance origin, while selected profile locations are labelled W11, W10, etc. Positive transport rates indicate transport toward the southeast. Positive transport divergence values indicate accretion. (a–c): Longshore transport rate for waves arriving from 15° east of north (wave thrust directed south-eastward), 55° east of north (wave thrust directed normal to the regional shoreline orientation), and 95° east of north (wave thrust directed north-westward). (d–e): Longshore transport rate and divergence for 8.5 second waves of various directions. Triangles on e show the loading pattern of the third principal component obtained from analysis of the 'whole shore' dataset (WS3). On all plots, points are omitted where the wave refraction analysis failed to provide acceptable breaking wave conditions (often, this occurred at profile W4, where a flood-tidal channel lay off the beach).

effects of storm-waves and swell on beach erosion and accretion, respectively. No such correlation was found for the near field compartments, indicating that the direct signature of the incident waves on cross-shore transport was masked by other processes which are later shown to relate to sand bars migrating from the ebb delta and to shifting flood-tidal channels.

Dispersion Diagrams

The patterns shown by the sub-reach volumes become clearer on the V^* dispersion diagram, which shows the changes with time at all of the ocean-facing profiles (Figure 9). This illustrates a marked contrast in the near- and far

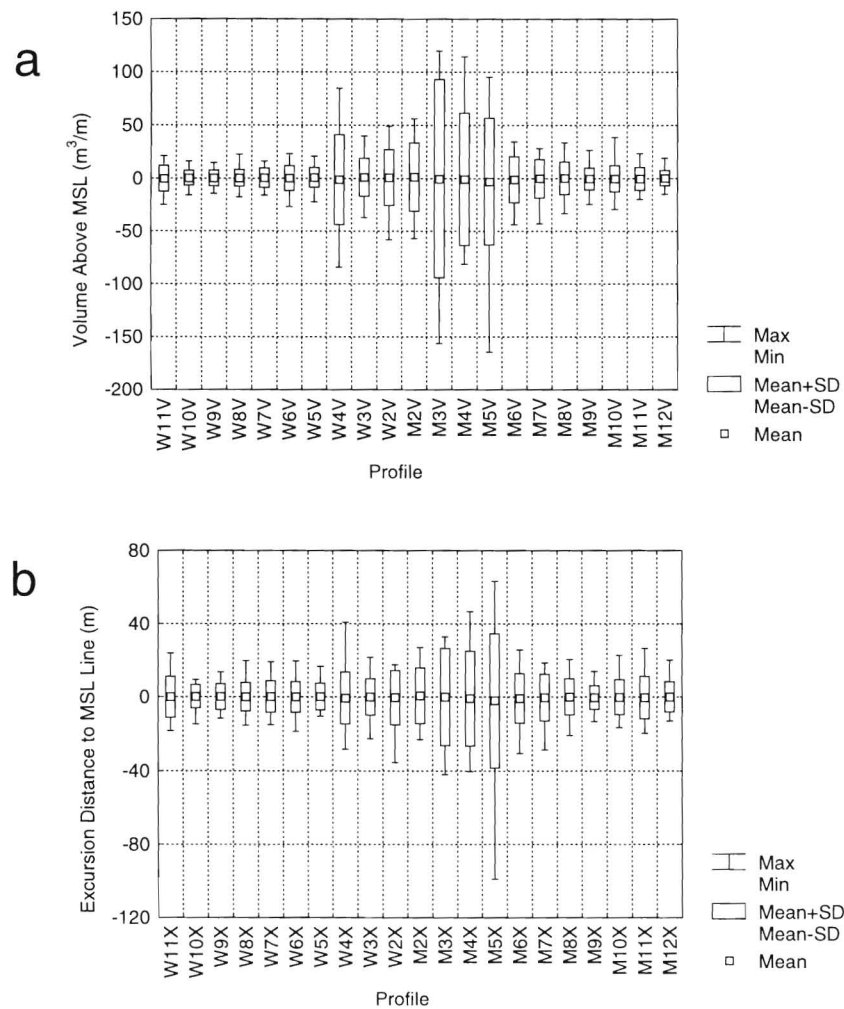


Figure 7. Plots showing range and standard deviation about mean values of (a) excursion volume above MSL datum and (b) excursion distance to MSL line at each of the open-ocean-facing profile locations over the study period.

field changes, and indeed suggests that the near field might be better defined extending between profiles W7 and M9. In the far field, the quasi-seasonal pattern of sand gains and losses shows up well (as 'horizontal morphology'). In contrast, in the near field the predominant features on the dispersion diagram run 'vertically', indicating features that span relatively short distances alongshore but persist in time. These patterns relate to the development of bars and holes spanning alongshore distances of about 500 m to several km and persisting for several years.

Some of these near field features appear to be fixed in position, at least over the time scale of the study, which probably relates to 'standing' effects on the waves and currents imposed by the general geometry of the ebb delta. Indeed, their position is consistent with the pattern of deposition and erosion predicted by the longshore-transport divergence analysis (Figure 6e)—for example, the trough-bar-trough pattern

fixed over profiles M5-M9 and the trough fixed over profiles W5-W7 (Figure 9).

Other near field features have migrated, as recorded by oblique 'morphology' on the dispersion diagram. A good example is the series of oblique 'troughs' and 'bars' that lie between profiles M2 and M8. These 'slope-up' to the left on the diagram, and are the signature of two sand bars and intervening troughs migrating westward towards the inlet. These features were also tracked by visual observation during the study period and are associated with the shoreward migration then welding of bars to the cusped foreland, which in turn forced the eastern marginal flood-tide channel to impinge against and scour the shore on the inlet side of the foreland. The consequent progressive loss of sand along this shore is clearly shown on Figure 9.

A similarly migrating trough was observed to move along the beach between W2 and W5 over the study period (its ap-

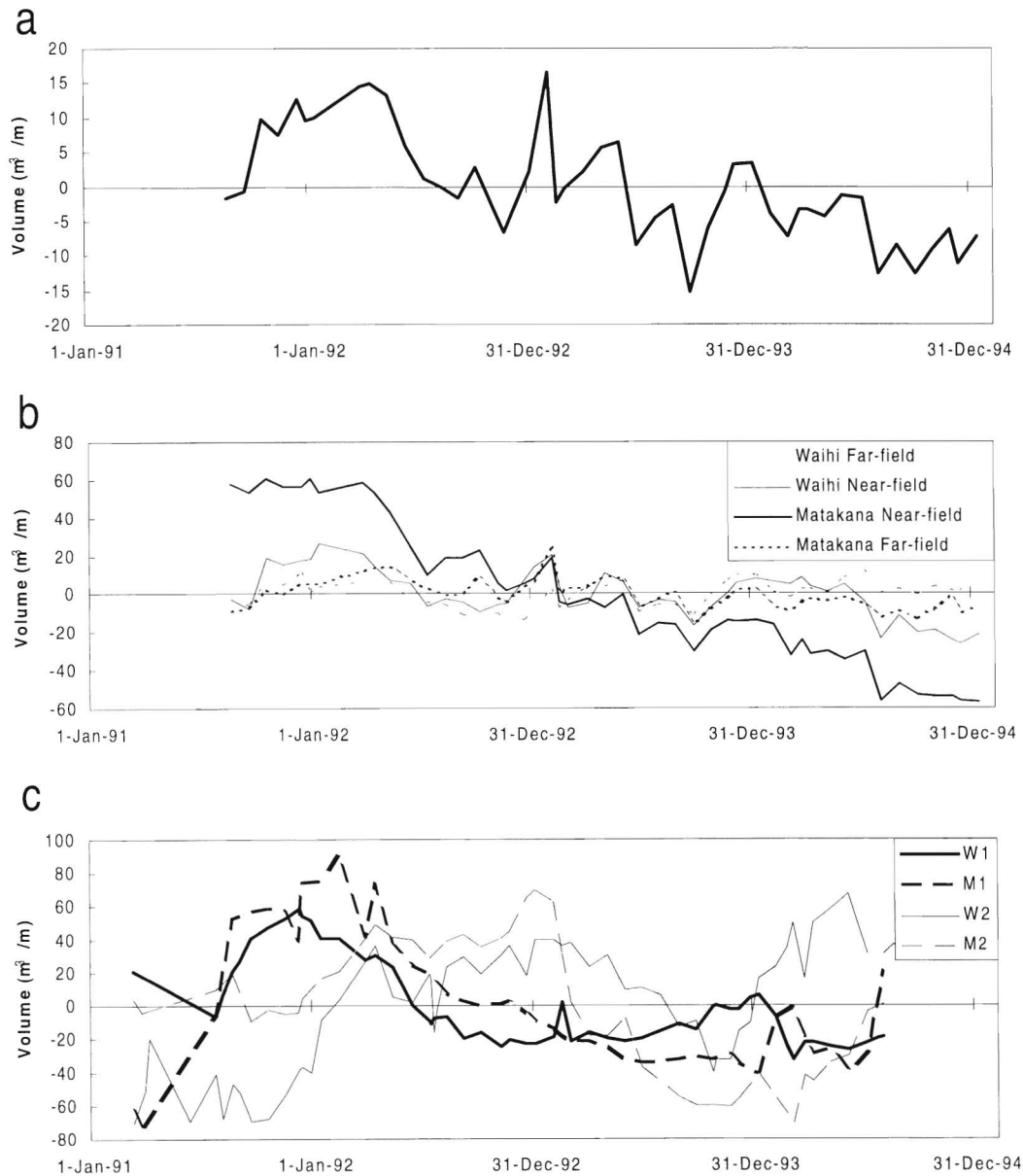


Figure 8. Changes in sand volume (per unit shore length) above MSL datum for (a) whole span of open-ocean-facing shore, (b) the four near- and far field compartments (see text for boundary definitions), and (c) the profiles within the inlet (W1 at Cave Bay and M1 inside the Matakana spit tip) and immediately beside the inlet (W2 and M2). All volumes are deviations from the mean values over the study period.

pearance on Figure 9 is partly masked by the superimposed quasi-seasonal changes). This trough was associated with shoreward migration of a sand bar from the ebb delta, which forced the western marginal flood channel to migrate shoreward and westward, scouring the beach as it migrated. Figure 9 records this migrating sand bar welding to the beach in the area of W2 in 1994.

The patterns along Waihi Beach also show the effect of the inter-annual fluctuation in net longshore transport (Figure 5d), which appears to have induced a migration of sand from

one end of Waihi Beach to the other. This appears on Figure 9 as a trend for erosion at the western end of the beach and accretion at the eastern end while the regional longshore transport was eastward (*e.g.*, mid 1991 through to late 1992), with the reverse trend occurring when the net transport was westward (1993 through 1994).

The erosion/accretion cycles prevalent in the far field regions of Figure 9 correlate reasonably well with the fall speed parameter signal (Figure 5b), confirming that they relate to storm-wave/swell driven cross-shore transport.

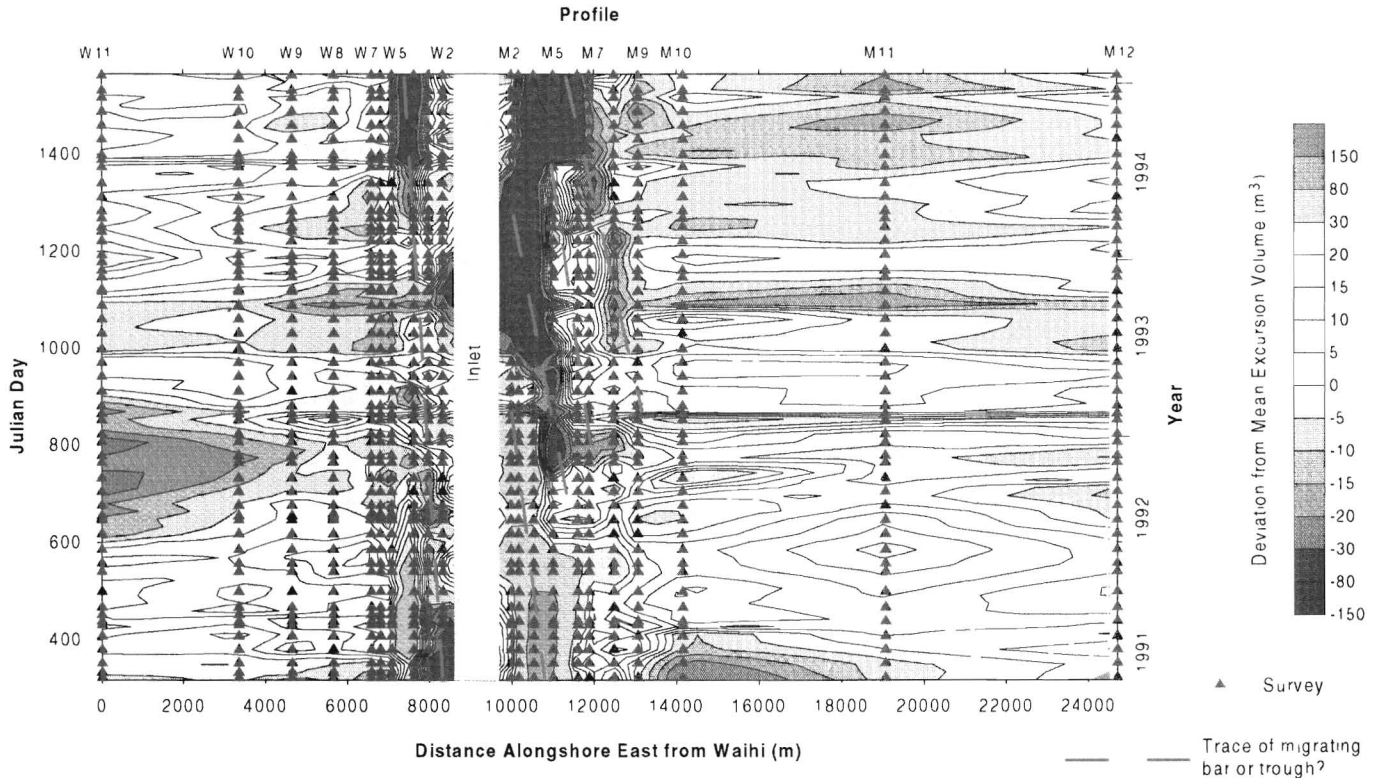


Figure 9. 'Dispersion diagram' showing alongshore patterns of change in sand volume (per unit shore length) above MSL datum over the study period. Triangles locate surveys of individual beach profiles. Dashed lines suggest the traces of alongshore-migrating erosion troughs and sand bars. The volumes are deviations from the mean values over the study period.

The equivalent dispersion diagrams for excursion distance, X^* , and for the rates of change of V^* and X^* lead to the same interpretations and so are not reproduced here.

Principal Components Analysis

Principal components analyses were conducted on the beach volume (V^*) data for each of the four sub-reaches and for the whole study shore. The sub-reaches were analysed separately to ensure that far field signals were not masked by the larger amplitude near field ones (e.g., see Figure 7). The longshore 'loadings' and 'scores' over time for the main principal components found for each reach of shore are plotted in Figure 10, while the correlations between the scores and the records of sub-reach volume, longshore transport potential, fall speed parameter, and mean sea level are listed in Table 1.

The principal components results varied among the sub-reaches. For the Waihi far field (WFF) sub-reach (profiles W11-W6), the three largest principal components explained 91% of the V^* variance. The first (WFF1, 63% variance) was in-phase all along the shore (i.e., when one profile gained or lost volume, all the others did the same) and showed a quasi-seasonal cycle that correlated significantly with the sub-reach volume and the fall speed parameter (Table 1, Figure 11a). This function clearly relates to changes on the sub-aerial beach associated with storm-waves and swell.

The second principal component (WFF2, 20% variance) showed a phase reversal alongshore and an approximately 3-year cycle that correlated very well with the cumulative longshore transport potential (Figure 11b). The longshore phase reversal indicates pivoting of sand gains/losses about a central nodal point. This function thus captures the sand migration reversals on Waihi Beach driven by inter-annual variations in the direction of net longshore transport observed in this study. WFF3 (explaining only 8% of the variance) is possibly the signature of a standing sand wave which induces subtle fluctuations in Waihi Beach's planform: during storms sand tends to converge alongshore towards the centre of the beach (straightening the shoreline overall) and during swell it returns to either end (increasing the shoreline curvature).

Along the Waihi near field (WNF) sub-reach (profiles W2-W5), the first three principal components (Figure 10b) contain 90% of the variance in V^* . The loadings of the first principal component (WNF1, 50% variance) indicate that W2 and W3 respond in opposite phase to W4 and W5, while the scores show a progressive increase with a superimposed inter-annual variation. This pattern is consistent with the visual record of a trough migrating slowly westward along this segment of shore through the study period, followed by the accretion of a sand bar in the region of W2-W3. The WNF1 scores correlate with the regional cumulative longshore

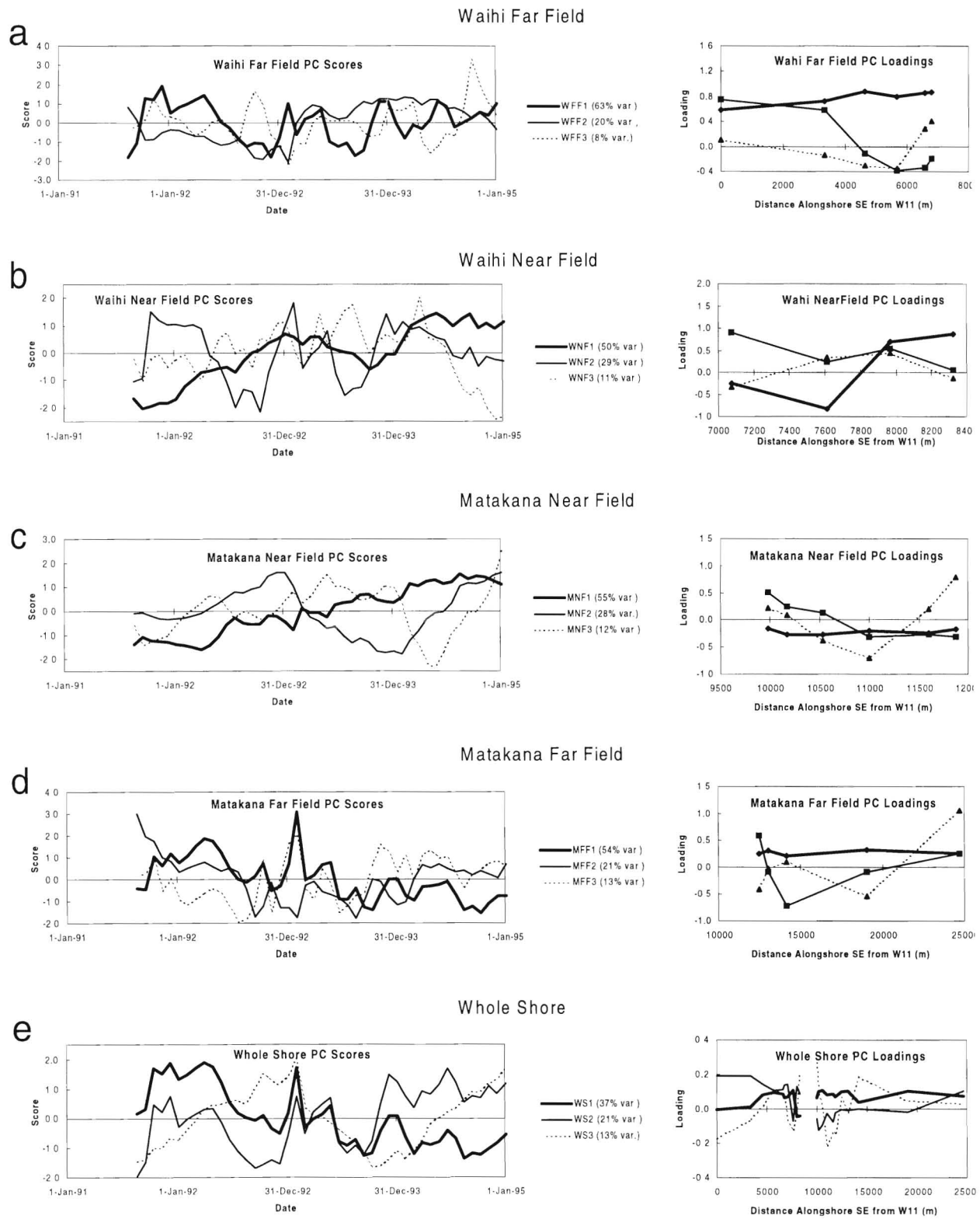


Figure 10. Temporal 'scores' and longshore 'loadings' for the three largest principal components for (a) Waihi Beach far field profiles, (b) Waihi Beach near field profiles, (c) Matakana Island near field profiles, (d) Matakana Island far field profiles, and (e) all open-ocean-facing profiles along the study shore. The % figures show the proportion of the total variance in sand volume explained by each principal component.

Table 1 Coefficients of correlation between principal components and wave forcing parameters and sand volume in sub-reaches. Asterisks mark correlations that are significant at the $p < 0.05$ level.

Reach	Principal component	% variance	Correlation coefficient with			
			Reach volume	Fall speed parameter	Cumulative longshore transport	28-day mean sea level
Waihi far field (W11-W6)	1	64	0.77 [*]	-0.47 [*]	0.18	0.15
	2	19	0.35 [†]	0.01	0.81 [‡]	-0.14
	3	7	0.03	0.10	0.09	0.18
Waihi near field (W5-W2)	1	50	0.38 [*]	0.07	0.46 [*]	-0.16
	2	29	0.57 [*]	0.43 [*]	0.26	0.04
	3	11	0.04	0.11	0.19	0.30
Matakana near field (M2-M7)	1	55	0.96 [‡]	0.23	0.76 [‡]	0.38 [*]
	2	28	0.07	0.13	0.29	-0.03
	3	12	0.20	0.06	-0.31 [†]	0.32
Matakana far field (M8-M12)	1	54	0.83 [‡]	0.44 [†]	0.57 [†]	0.48 [‡]
	2	21	0.21	0.04	0.35 [†]	0.24
	3	15	0.18	0.16	0.46 [†]	0.14
Whole shore (W11-M12)	1	37	0.73 [†]	0.40 [†]	0.54 [†]	0.41 [†]
	2	21	0.06	0.36 [†]	0.69 [‡]	0.01
	3	13	0.22	0.03	-0.33 [*]	0.03

transport signal (Table 1). The sign of this correlation suggests that W4 and W5 tended to accrete and W2 and W3 to erode when the net regional transport was eastward (and vice-versa when the transport was westward). This longshore transport influence may arise from a combination of effects: wave refraction causing longshore transport divergence (Figure 6e); an extension of the sand 'sloshing' between the two Waihi Beach headlands; and sand losses into the inlet during eastward transport conditions.

WNF2 (29% variance) had loadings in-phase alongshore and showed a quasi-annual cycle which correlated both with the fall speed parameter and the sub-reach sand volume (Table 1). This clearly relates to cross-shore transport effects associated with storm and swell waves. The notable difference with the Waihi far field, though, is that in the near field this cross-shore transport factor is subordinate to other effects. The near-zero loading of WNF2 at W2, nearest the inlet, suggests that this incident wave signal diminishes progressively in the lee of the ebb delta. WNF3 (11% variance) may capture the welding to the beach in 1994 of the sand bar that had been migrating shoreward from the delta margin.

For the Matakana near field (MNF) sub-reach (profiles M2-M7), the three largest principal components (Figure 10c) explained 95% of the variance in V^* . The first (MNF1, 55% variance) had loadings in-phase alongshore and showed a progressive decrease in V^* with time. This pattern is consistent with the progressive erosion observed to accompany the migration toward the inlet of a scour hole associated with the eastern marginal flood-tidal channel, as described earlier. MNF1 correlated well with the sub-reach sand volume and with the cumulative regional longshore transport (Figure 11c and Table 1). The latter correlation involves a decrease in beach sand volume associated with westward transport, suggesting that easterly (of normal) waves tended to drive Matakana Beach sand into the inlet entrance from where it was caught in the tidal flows then recirculated out onto the ebb delta.

MNF2 (28% variance) had the inlet end of the sub-reach

eroding while the eastern end accreted, and varied over something like a 2-year time scale. This had no significant correlation with any of the forcing functions, although a significant correlation with the cumulative longshore transport ($r = -0.63$) was achieved after a 6 month lag. This suggests a signal linked to sand accumulation on swash bars offshore on the ebb delta platform. The original sand deposition would be associated with longshore transport events but it would require of the order of 6 months for it to translate shoreward and affect the beach. MNF3 (12% variance), showing another 'centrally inverted' loading and an irregular time series, appears to capture the welding of a sand bar to the cusped foreland (in the area of profiles W4 and W5) during 1994. The MNF3 scores correlate significantly with the cumulative longshore transport potential after a 12 month lag. Again, this suggests that the beach accretion was initiated by an earlier longshore-transport-linked deposition event on the delta platform, with a lag period required to translate this bar form shoreward onto the beach.

A key feature of these Matakana near field principal components is that they all involved inter-annual to longer time scales. None correlated with the seasonal storm-wave/swell signal. This is consistent with the Matakana near field beaches being well protected from waves from the N-NE by the ebb delta bars.

For the Matakana far field (MFF) sub-reach (profiles M8-M12), the three largest principal components (Figure 10d) explained 88% of the variance in V^* . The MFF1 (54% variance) loadings were in-phase alongshore, and the scores showed a quasi-seasonal fluctuation which correlated with the sub-reach sand volume and the fall speed parameter (Table 1). As at Waihi Beach, this indicates the predominance of the incident waves. MFF1 also correlated significantly with the cumulative longshore transport (Table 1), indicating accretion during episodes of eastward transport and erosion with westward transport. The latter connection is suggestive of westerly-directed waves driving sand from the beach into the inlet. Easterly-directed waves may simply stop this pro-

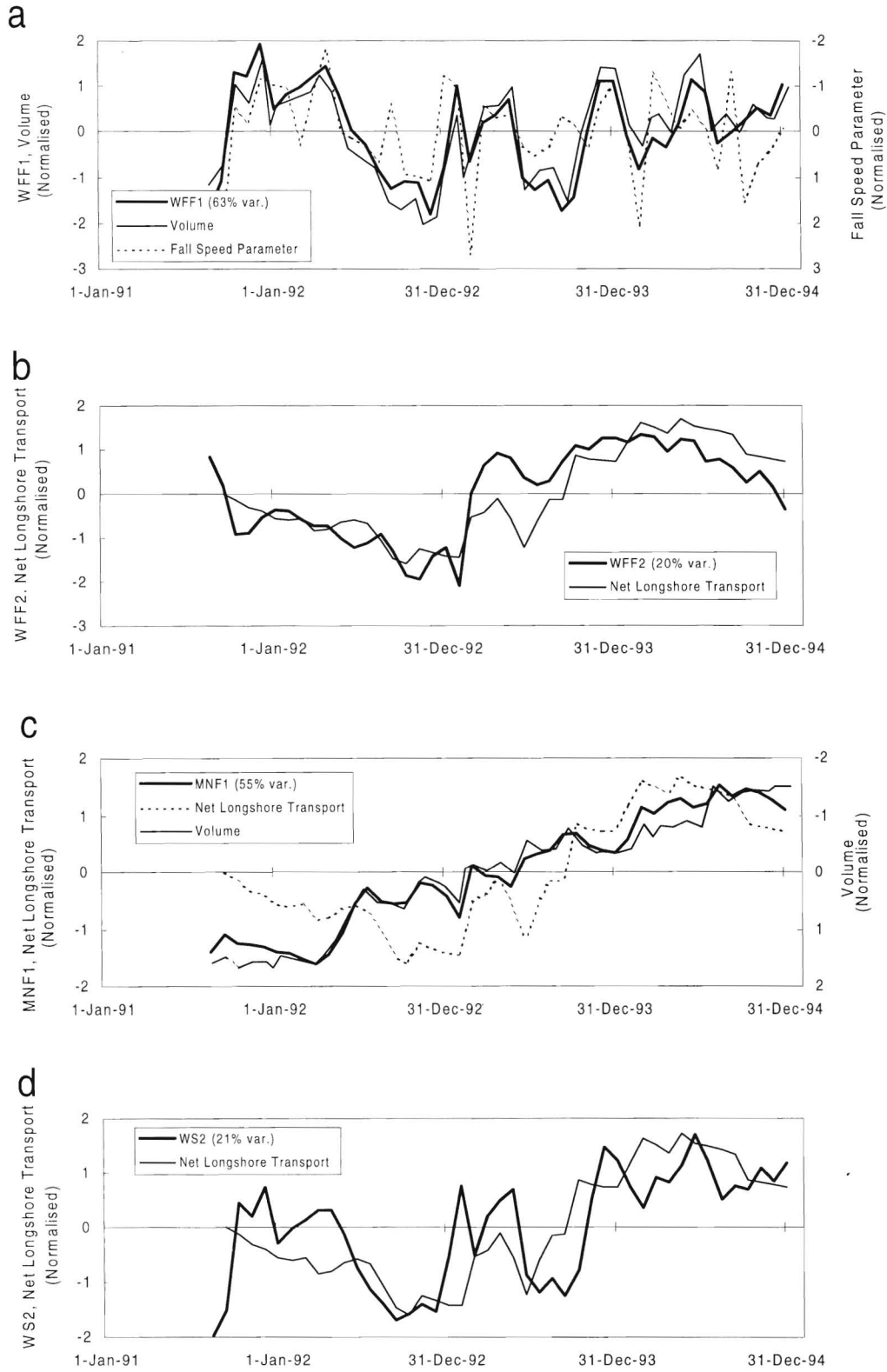


Figure 11. Selected principal components time-series (scores) overlaid on various forcing function and beach volume time-series. (a) Waihi Beach far field first principal component (WFF1) and beach volume with fall speed parameter, (b) Waihi Beach far field second principal component (WFF2) with net regional longshore transport, (c) Matakana Island near field first principal component (MNF1) and beach volume with net regional longshore transport, and (d) whole-shore second principal component (WS2) with net regional longshore transport.

cess. Our wave refraction analysis (Figure 6) suggests that no significant 'drumstick' effect (*i.e.*, whereby transport would stall on the downdrift side of the ebb delta due to wave refraction effects) occurs this far alongshore with easterly-directed waves.

The MFF2 and MFF3 (21% and 13% of variance, respectively) loadings vary in sign alongshore, showing patterns suggestive of discontinuous sand bars. The MFF2 scores suggest a 3-4 year cycle and correlate weakly but significantly with the cumulative longshore transport (Table 1). A much better correlation with the longshore transport is achieved ($r = -0.72$) after a 14 month lag, suggesting that this signal is associated with the effect of longshore transport on offshore bars, possibly associated with bar-bypassing around the ebb delta margin. The correlation of the more irregular MFF3 scores with the longshore transport does not improve notably after a lag period, suggesting a direct influence of obliquely incident waves on the beach volume. Possibly, this signal relates to offshore bar effects on wave refraction.

As anticipated, the principal components analysis was less successful at separating variance in V^* along the whole length of open-ocean-facing shore (the first three components explained 71% of the variance) due to the weighting effect of the more closely spaced near field profiles. Nonetheless, the first whole-shore principal component (WS1, 37% variance) patterns do suggest something like a 3-4 year cycle of beach change involving the near field of the ebb delta and the Matakana far field. The WS1 scores correlated well with the record of beach volume weighted by profile spacing, but since they also correlated significantly with all of the forcing functions, the cause of the overall beach volume change is confused. Most likely, the cycle captured by WS1 reflects the long-term circulation of sand between the beaches and the ebb delta. The loadings of WS2 (21% variance) are weighted to Waihi Beach and M12 on Matakana Island, and its scores correlate well with the cumulative longshore transport (Figure 11d) and less so with the fall speed parameter (Table 1). This appears to represent several far field effects, such as reversing sand migrations and the quasi-annual storm-wave influence. WS3 (13% variance) has a loading pattern very similar to the transport divergence pattern found from the refraction analysis (Figure 6e), and its scores show a reasonably distinct 2-year cycle and correlate only with the cumulative longshore transport. WS3, then, appears to represent the consequences of the ebb delta's interruption of the regional longshore transport field. The WS3 loading pattern suggests that this effect might extend as far west from the inlet as W9 and as far east as M11—further than suggested by the refraction analysis.

DISCUSSION

Scales of Coherent or Similar Change

The above results depict clear differences in the spatial and temporal scales of sand volume and shoreline change on beaches behind and adjacent to the Katikati ebb delta. The near field changes are larger and mainly occur over multi-year time scales, either in phase with (or lagging) inter-annual fluctuations in the direction of net longshore transport

or in association with morphologic change on the ebb delta bar/channel systems or with bars migrating shoreward off the delta and welding to the beach. Day to day, storm to storm beach changes associated with the incident wave conditions are small compared with these longer-term changes.

This contrasts with the far field situation where the primary beach changes show storm to seasonal time scales and are phase-locked to the incident wave conditions. These changes reflect variations in wave steepness and correspond to cross-shore sand exchanges between the sub-aerial beach and offshore bars. Lesser far field changes are linked to inter-annual variations including sand migration from one end of a headland-bound beach to another and sand 'pumping' from the beaches into the inlet/ebb-delta system.

The spatial scales of change found in this study are consistent with those reported by FENSTER and DOLAN (1996) from mixed energy, tide dominated natural inlets on the Virginia barrier islands. Using rate-of-change of shoreline position to define the extent of inlet effects on adjacent beaches, they found that inlet effects dominated shoreline changes up to 4.3 km from the inlet and exerted lesser influence up to 6.8 km updrift and 5.4 km downdrift. At Katikati, inlet dominance, defined in terms of the magnitude of the shoreline fluctuations (Figure 7), spanned approximately 2 km either side of the inlet. However, by considering temporal patterns of change as well (*e.g.*, Figure 9), it is clear that the span of influence extended for 3-4 km on the eastern (Matakana) side and 2.5 km on the western (Waihi) side. Since the tidal prism of Katikati Inlet is $0.95 \times 10^8 \text{ m}^3$ while the tidal prisms of FENSTER and DOLAN's Virginia inlets ranged from $2.6-5.6 \times 10^8 \text{ m}^3$, and since ebb delta size is proportional to tidal prism volume to the power of 1.4 (HICKS and HUME, 1996), we would expect that the linear scales at Katikati inlet would be approximately $(0.95/5.6)^{1/4 \cdot 0.33} = 0.44$ times the largest reported by FENSTER and DOLAN, which is so. Although our approach differed from FENSTER and DOLAN's in that we analysed normalised changes in beach volume and shoreline position, since the time steps between our surveys were reasonably uniform (averaging one month) this is essentially the same as working with the integral of the rates of change.

Inlet and Ebb Delta Near-field Effects

The tidal inlet and ebb delta system at Katikati affect the near field shore through a number of processes. These include wave sheltering, localised wave focusing, scour by flood-tidal channels, bar migration and welding, and divergence in the longshore transport due to wave refraction. Over time scales of several years, these processes produce a superposition of positionally fixed, migrating, and transient shore features.

Wave Sheltering

The ebb delta, with its broad dissipative platform areas, marginal bars, and obliquely-inclined rows of linear bars presents an effective breakwater for the near field beaches within its lee. This sheltering is substantial along the Matakana shore between the inlet and the cusped foreland, at least as regards erosion due to offshore transport. The main direct effect of incident waves on this shore appears to be easterly

waves driving sand alongshore towards the inlet throat. A storm wave signal was recognizable on the Waihi near field beaches. However, the principal components analysis showed that this storm wave erosion was subordinate to the effects of longshore transport and bar/channel migration and that it diminished towards the inlet, almost disappearing at profile W2. Locally and for irregular periods, where gaps developed in the system of offshore bars or wave field distortion occurred over the bar/channel topography of the ebb delta flanks, more wave energy reached the beach and transient scour holes developed (*e.g.*, Figure 3).

Generally, at least over the four years of the study, the broad extent of the wave sheltering effect appeared to be fixed in space by the shape of the delta. Major changes in the ebb delta shape made by large rare storms would alter this pattern of wave protection, thus inducing a long-term cycle of near field beach change while the ebb delta recovered its normal shape. HUME *et al.* (in preparation) describe the Katikati ebb delta being "flattened against the shore" during major storms in 1975 and 1982, inducing decadal-scale variations in the ebb delta shape. FITZGERALD and NUMMEDAL (1983) described cyclical episodes of bar growth on the ebb delta at Price Inlet, South Carolina, which led to varying exposure to wave energy and varying beach erosion.

Moving Flood-Tidal Channels, Accreting Bars, and Sand Circulation

Flood-tidal channels and bars migrating shoreward from the ebb delta platform were major influences on the near field beach changes recorded at Katikati. Erosion occurred when bars on the ebb delta platform forced the flood-tidal flow close against the beaches. This erosion was maximised on the Matakana side of the inlet during episodes of energetic easterly waves, when the flood current and the highly obliquely incident waves combined to scour the beach face and drive sand towards the inlet throat. Changes in the position, orientation, and degree of development of the flood channels followed from changes in the bar patterns, which in turn were linked to the wave conditions. After a bar migrated shoreward and welded to the beach, the flood channel tended to reform seaward of the bar and the beach passed into an accretionary phase.

These near field erosion/accretion cycles are the shoreline signature of sand circulation cells within the inlet/ebb-delta system. In these, sand is circulated at intervals from temporary storage on the near field beaches, moving via the flood channels and the main ebb channel, to storage on bars flanking the ebb channel and around the delta margins. The loop is closed when the bars migrate shoreward, often as bar complexes, to weld to the near field beach (see HUME *et al.*, in preparation, for details). This latter stage is the slowest and appears to be the main control on the time scale of the cycle. However, the history of wave conditions also matters, since this determines the modification of bars and bar complexes and their rate and direction of migration. Large storms, which can quickly create new bar features and induce shifts in the main ebb channel, can interrupt or accelerate the cycle. Also, variations in the wave direction and the prevailing direction of longshore transport (Figure 5d) mean that the sand

circulation cells on either side of the inlet may be independent. A conceptual model of sand transport paths around the Katikati ebb delta under different wave directions is given in HUME *et al.* (in preparation). Similar processes have been described at mixed energy inlets elsewhere (*e.g.*, FITZGERALD, 1988).

From this study and from inspection of earlier aerial photographs, the time frame of the Katikati cycles appears to be typically about 4–5 years. Their longshore extent depends on the length of bars shed by the ebb delta. During our study bar accretion occurred at the cusped foreland, but HUME *et al.*'s (in preparation) historical record indicates that bars come onshore up to 3 km further south-east (*i.e.*, as far as profile M10 on Figure 1).

Longshore Transport Divergence

Our investigation of the divergence induced in the regional longshore transport field by wave refraction over the submerged ebb delta predicted a divergence pattern that was remarkably similar for a wide range of incident wave directions (Figure 6e). This essentially standing effect indicated deposition very close to the inlet on both sides then erosion holes extending alongshore for approximately 3 km. The principal components analysis suggested that this effect was indeed occurring, waxing and waning according to the regional longshore transport potential, but was partly masked by other processes such as bar and channel migration. These would tend to smooth-out the shoreline perturbations that would otherwise develop from the transport divergence pattern.

Figure 6e shows that the transport divergence effect spanned some 9–10 km between profiles W10 and M10. This extends well into what we have defined as the far field, emphasizing that the wave field is distorted by the whole area of submerged ebb delta, not just the shallow platform area that is easily visible on air photographs (the bathymetric signature of the Katikati ebb delta extends offshore to about the 20 m isobath and spans some 6–7 km alongshore—HICKS and HUME, 1997).

There is no indication on Figure 6e that littoral transport divergence is the cause of the drumstick shape of the Matakana Island barrier. This appears to be more to do with the attachment of bars at the cusped foreland. Possibly when this foreland is in a more accreted state than it was during our study (when the bathymetry for the refraction analysis was surveyed), it would induce a different divergence pattern involving more extensive sand trapping. At that state, too, one would expect more bar-bypassing of sand around the delta. During most of our study, the foreland was not particularly accreted and extended periods of easterly waves kept it so, trimming sand off the foreland and pumping it into the inlet.

Far Field Effects: Shoreline Pivoting, Littoral Drift Capture and Bypassing

Although much of the far field beach change was associated with storm waves and cross-shore sand transport, the longshore transport regime also induced change. Different mechanisms dominated the longshore transport effect on opposite

sides of the inlet. On Waihi Beach, the inter-annual reversals in the net regional longshore transport potential appeared to induce sand migration between the Waihi and Bowentown headlands, which caused the Waihi shoreline to subtly pivot over inter-annual time periods.

On Matakana Island, the far field beach showed a weak trend of sand loss superimposed on the storm-swell induced changes. Net sand losses appeared to be associated with episodes of intense westward transport (compare Figures 5e and 8b). This westward transport continued through the Matakana near field, being most intense on the inlet side of the cusped foreland (Figure 6c), with the sand eventually being pumped into the inlet. Once trapped in the inlet, the sand was routed to the ebb delta and was not immediately available to be returned to the beaches when the transport direction reversed. Thus in this respect, at least on a storm by storm basis, the inlet/delta system functions as a 'non-return valve' for beach sand, and erosion can accumulate on the beaches for several years before a sand bar eventually migrates onshore from the ebb delta and a sand slug is released alongshore. Thus by this sand pumping process the inlet/delta system can induce a multi-year pattern on the far field beach. This effect should extend well alongshore, since, unlike sand piling up against a headland (which changes the shoreline orientation and longshore transport efficiency), the inlet and its strong tidal currents are more than capable of clearing the sand fed to it by the littoral conveyor belt.

Littoral drift bypassing can also contribute to far field beach change if the bypassing occurs through a mechanism that amplifies discontinuities in the supply of sand to the downdrift beaches. This is more likely where 'tidal bypassing' is the main bypassing mechanism, since this essentially transforms a relatively steady inflow of littoral drift into a discontinuous supply of sand packets. With this, the downdrift beach might be expected to experience cycles of erosion and accretion phase-locked to the bypassing cycle, although probably damped in size and lagged in time further away from the inlet. HUME *et al.* (in preparation) show that Katikati inlet is indeed mainly a 'tidal bypasser' (although 'bar bypassing' also tends to occur under northerly wave conditions). However, they class it as a "poor bypasser", since much of the sand moving off the delta tends to be recirculated rather than leak alongshore to the downdrift beaches (this is not surprising given that the net drift at Katikati is essentially oscillatory over inter-annual time scales). Thus large obvious shoreline fluctuations associated with bypassed sand slugs are not expected along the study shore, and we would be unlikely to observe them over the time scale of our study.

CONCLUSIONS

The main conclusions of this study of a large mixed-energy ebb delta and its adjacent beaches are:

- (1) Changes to sand volume and shoreline position on near field beaches were 3–4 times larger than on the far field beaches.
- (2) Changes on the far field beaches were dominated by cross-shore transport associated with alternating storm and swell episodes that showed a weak quasi-annual cycle. Small-

er far field changes were linked with longshore transport at inter-annual time scales. The longshore transport was manifest as sand migration reversals between the small headlands bounding the western beach and pumping of beach sand into the inlet/ebb delta system from either side.

- (3) On the near field beaches, erosion due to storm waves was severely damped by the breakwater action of the ebb delta. The predominant near field beach changes occurred at multi-year time scales and related mainly to the shoreward migration of sand bars off the ebb delta and scouring by the marginal flood-tidal flows as these were deflected and forced to migrate by sand bar activity on the delta. These changes were the on-shore signature of a cycle of sand circulation between the beaches and the ebb delta bars.

- (4) Beach sand is regularly pumped into the inlet by tidal currents and oblique wave thrust but is returned only infrequently in packets as sand bars which migrate back to the beach from the delta. Whether associated simply with a closed loop of sand circulation or a 'leaky loop' that involves littoral drift bypassing, this transformation of time scale between the sand inflows and outflows induces multi-year alternations of sand deficit or surplus on the adjacent beaches.

- (5) Wave refraction over the submerged ebb delta created much the same pattern of longshore transport divergence irrespective of the incident wave direction. This resulted in a standing pattern of transport-divergence induced beach erosion and accretion about the inlet. This effect was largest on the near field beaches, particularly on the eastern side, but extended several km alongshore beyond the easily visible margins of the ebb delta.

- (6) The contrasting magnitudes, time scales, and causes of near- and far field beach changes should be heeded when defining coastal-erosion hazard zones along coasts with tidal inlets. For situations similar to Katikati, several decades of observation with adequate spatial detail are required to capture the changes induced in the adjacent beaches by the inlet/ebb-delta system.

ACKNOWLEDGEMENTS

We wish to thank NIWA Hamilton staff for field and data processing support, particularly R.K. Smith and R.O. Oven-den for the beach profile work, and Dr. J.G. Gibb for a constructive review of the manuscript. The study was funded by the New Zealand Foundation for Research, Science and Technology under contract number CO1211.

LITERATURE CITED

- AUBREY, D.G. 1979. Seasonal patterns of on/offshore sediment movement. *Journal of Geophysical Research*, 84, 6347–6354.
- BELL, R.G. and GORING, D.G. 1996. Techniques for analyzing sea level records around New Zealand. *Marine Geodesy*, 19, 77–98.
- BRUNN, P. 1954. Migrating sand waves or sand humps, with special reference to investigations carried out on the Danish North Sea coast. *Proceedings of the 5th Coastal Engineering Conference* (ASCE, Grenoble), pp. 269–294.
- BRUNN, P. 1962. Sea level rise as a cause of shore erosion. *Journal of Waterways and Harbours Division*, 88(WW1), 117–130.
- BRUNN, P. 1990. Morphological and navigational aspects of tidal inlets on littoral drift shores. *Journal of Coastal Research*, 2, 123–145.

- CERC 1984. *Shore Protection Manual*. Coastal Engineering Research Centre, U.S. Army Corps of Engineers, Waterways Experiment Station.
- DEAN, R.G. 1973. Heuristic models of sand transport in the surf zone. *Proceedings of the Conference on Engineering Dynamics in the Surf Zone* (Sydney, Australia), pp. 208–214.
- DAVIS, R.A. Jr., HUME, T.M., and HICKS, D.M., in preparation. Geomorphology and classification of 'flood tidal deltas' in a headland dominated, active margin, coastal setting. Submitted to *Journal of Coastal Research*.
- DOLAN, R. 1970. Sand waves, Cape Hatteras, North Carolina. *Shore and Beach*, April 1970, 23–25.
- DOLAN, R.; HAYDEN, B.P., and SHABICA, S.V. 1982. Beach morphology and inshore bathymetry of Horn Island, Mississippi. *Journal of Geology*, 90, 529–544.
- EBERSOLE, B.A.; CIALONE, M.A., and PRATER, M.D. 1986. Regional Coastal Processes Numerical Modelling System. Report 1. RCPWAVE—A Linear Wave Propagation Model for Engineering Use. *Technical Report CERC-86-4*, Coastal Engineering Research Center, U.S. Army Corps of Engineers, Vicksburg, Mississippi.
- EMERY, K.O. 1961. A simple method for measuring beach profiles. *Limnology and Oceanography*, 6, 90–93.
- EWART, A. 1961. Review of mineralogy and chemistry of acidic volcanic rocks of the Taupo volcanic zone New Zealand. *Bulletin of Volcanology*, 29, 147–171.
- FENSTER, M. and DOLAN, R. 1996. Assessing the impact of tidal inlets on adjacent barrier island shorelines. *Journal of Coastal Research*, 12, 294–310.
- FITZGERALD, D.M. 1984. Interactions between the ebb tidal delta and landward shoreline: Price Inlet, South Carolina. *Journal of Sedimentary Petrology*, 54, 1303–1318.
- FITZGERALD, D.M. 1988. Shoreline erosional-depositional processes associated with tidal inlets. In: D.G. AUBREY and L. WEISHAR (eds), *Hydrodynamics and Sediment Dynamics of Tidal Inlets, Lecture Notes on Coastal and Estuarine Studies*, 29. New York, Springer-Verlag, pp. 186–225.
- FITZGERALD, D.M. and NUMMEDAL, D. 1983. Response characteristics of an ebb-dominated inlet channel. *Journal of Sedimentary Petrology*, 53, 833–845.
- FITZGERALD, D.M.; FICO, C., and HAYES, M.O. 1979. Effects of the Charleston Harbor, South Carolina, jetty construction on local accretion and erosion. *Proceedings of the Speciality Conference on Coastal Structures*, 79 (ASCE, Alexandria, Virginia), pp. 641–644.
- FITZGERALD, D.M. and HAYES, M.O. 1980. Tidal inlet effects on barrier island development. *Proceedings of Coastal Zone '80* (ASCE, Hollywood, Florida), pp. 2355–2379.
- GIBB, J.G. 1977. Late Quaternary sedimentary processes at Ohiwa Harbour, Eastern Bay of Plenty with special reference to property loss on Ohiwa Spit. *Water & Soil Technical Publication No. 5*, Water & Soil Division, Ministry of Works and Development, Wellington, 16p.
- GIBB, J.G. 1994. Initial assessment of areas sensitive to coastal hazards for selected parts of the Bay of Plenty coast. *Consultancy Report CR94/17* for Bay of Plenty Regional Council, Tauranga, New Zealand, 36p+app.
- GIBEAUT, J.C. and DAVIS, R.A. Jr. 1993. Statistical geomorphic classification of ebb-tidal deltas along the west-central Florida coast. *Journal of Coastal Research*, 18, 165–184.
- GOLDEN SOFTWARE 1994. SURFER for Windows Reference manual. Golden Software, Inc., Golden, Colorado.
- GORING, D.G. and BELL, R.G. 1996. Distilling information from patchy tide gauge records: The New Zealand experience. *Marine Geodesy*, 19, 63–76.
- GRAVENS, M. B.; KRAUS, N.C., and HANSON, H. 1991. GENESIS: Generalized model for simulating shoreline change. Report 2, "Workbook and system user's manual", Technical Report CERC-89-19, U.S. Army Waterways Experiment Station, Coastal Engineering Research Center, Vicksburg.
- GREEN, M.O. 1994. Regional Coastal Processes Wave Propagation Model (RCPNIWA): User's Manual. *NIWA Internal Report IR94/05*, NIWA, Hamilton, New Zealand, 70p+app.
- HANSON, H. and KRAUS, N.C. 1989. GENESIS: Generalized model for simulating shoreline change. Report 1, "Technical Reference", Technical Report CERC-89-19, U.S. Army Waterways Experiment Station, Coastal Engineering Research Center, Vicksburg.
- HARRAY, K.G. 1976. *Beach erosion and sediments at Waihi Beach*. Unpublished MSc thesis, University of Waikato, New Zealand, 79p.
- HARRAY, K.G. and HEALEY, T.R. 1978. Beach erosion at Waihi Beach, New Zealand. *Journal of Marine and Freshwater Research*, 12, 99–107.
- HASHIMOTO, H. and UDA, T. 1982. Field investigation of beach profile changes and the analysis using empirical eigen functions. *Proceedings of the 18th Coastal Engineering Conference* (ASCE), pp. 1369–1384.
- HAYES, M.O., 1979. Barrier island morphology as a function of tidal and wave regime. In: LEATHERMAN, S.P., (ed.), *Barrier Islands: From the Gulf of St Lawrence to the Gulf of Mexico*. New York: Academic, pp. 1–28.
- HAYES, M.O. and KANA, T.W. 1976. Terrigenous clastic depositional environments. *Technical report No. 11*, CRD, Department of Geology, University of South Carolina, Columbia, South Carolina, 364p.
- HICKS, D.M. and INMAN, D.L. 1987. Sand dispersion from an ephemeral river delta on the Central California Coast. *Marine Geology*, 77, 305–318.
- HICKS, D.M. and HUME, T.M. 1996. Morphology and size of ebb-tidal deltas at natural inlets on open-sea and pocket-bay coasts, North Island, New Zealand. *Journal of Coastal Research*, 12, 47–63.
- HICKS, D.M. and HUME, T.M. 1997. Determining sand volumes and bathymetric change on an ebb-tidal delta. *Journal of Coastal Research*, 13(2), 407–416.
- HUME, T.M. and HERDENDORF, C.E. 1992. Factors controlling tidal inlet characteristics on low drift coasts. *Journal of Coastal Research*, 8, 2, 355–375.
- HUME, T.M.; HICKS, D.M.; SMITH, R.K., and DOLPHIN, T.J. in preparation. Ebb-tidal delta morphodynamics at a headland-barrier inlet in a mixed energy (tide-dominated) coastal setting, Katikati Inlet, New Zealand. Submitted to *Journal of Coastal Research*.
- KOMAR, P.D. and INMAN, D.L. 1970. Longshore sand transport on beaches. *Journal of Geophysical Research*, 73, 30, 5914–5927.
- LARSON, M. and KRAUS, N.C. 1989. SBEACH: Numerical model for simulating storm-induced beach change. Report 1, "Empirical foundation and model development", Technical Report CERC-89-9, Coastal Engineering Research Center, U.S. Army Corps of Engineers, Vicksburg, Mississippi.
- MACKY, G.H.; LATIMER, G.J., and SMITH, R.K. 1995. Wave observations in the western Bay of Plenty, New Zealand, 1991–94. *New Zealand Journal of Marine and Freshwater Research*, 29, 311–328.
- MEDINA, R.; LOSADA, M.A.; DALRYMPLE, R.A., and ROLDAN, A. 1991. Cross-shore sediment transport determined by EOF method. *Coastal Sediments '91* (ASCE), pp. 2160–2174.
- MUNROE, A.J., 1994. *Holocene evolution and palaeolimnology of a barrier spit, northwestern Matakana Island, Bay of Plenty, New Zealand*. Unpublished MSc thesis, University of Waikato, New Zealand, 172p.
- NUMMEDAL, D. and FISCHER, I., 1978. Process-response models for depositional shorelines: The German and Georgia Bights. *Proceedings of the 16th Coastal Engineering Conference*, pp. 1215–1231.
- SMITH, J.B. and FITZGERALD, D.M., 1994. Sediment transport patterns at the Essex River Inlet ebb-tidal delta, Massachusetts. *U.S.A. Journal of Coastal Research*, 10, 752–774.
- STATSOFT. 1991. STATISTICA Reference Manual. Statsoft, Tulsa, Oklahoma.
- WALTON, T.L., JR. and ADAMS, W.D. 1976. Capacity of inlet outer bars to store sand. *Proceedings of the 15th Conference on Coastal Engineering* (ASCE, New York), 2, 1919–1937.
- WILLIAMS, B.L. and BELL, R.G. 1991. Bay of Plenty oceanographic survey. *Water Quality Centre Report 6130/1*, Ministry of Works and Development, Hamilton, New Zealand, 38p.
- WINANT, C.D.; INMAN, D.L., and NORDSTROM, C.E. 1975. Description of seasonal beach changes using empirical eigenfunctions. *Journal of Geophysical Research*, 80, 1979–1986.